Different Flavors of Nonadiabatic Molecular Dynamics

Federica Agostini,* Basile F. E. Curchod†

March 15, 2019

Article Type:

Overview

Abstract

The Born-Oppenheimer approximation constitutes a cornerstone of our understanding of molecules and their reactivity, partly because it introduces a somewhat simplified representation of the *molecular wavefunction*. However, when a molecule absorbs light containing enough energy to trigger an electronic transition, the simplistic nature of the molecular wavefunction offered by the Born-Oppenheimer approximation breaks down as a result of the now non-negligible coupling between nuclear and electronic motion, often coined *nonadiabatic couplings*. Hence, the description of nonadiabatic processes implies a change in our representation of the molecular wavefunction, leading eventually to the design of new theoretical tools to describe the fate of an electronically-excited molecule. This Overview focuses on this quantity – the total molecular wavefunction – and the different approaches proposed to describe theoretically this complicated object in non-Born-Oppenheimer conditions, namely the Born-Huang and Exact-Factorization representations. The way each representation depicts the appearance of nonadiabatic effects is then revealed by using a model of a coupled proton-electron transfer reaction. Applying approximations to the formally exact equations of motion obtained within each representation leads to the derivation, or proposition, of different strategies to simulate the nonadiabatic dynamics of molecules. Approaches like quantum dynamics with fixed and time-dependent grids, traveling basis functions, or mixed quantum/classical like surface hopping, Ehrenfest dynamics, or coupled-trajectory schemes are described in this Overview.

*Laboratoire de Chimie Physique, UMR 8000 CNRS/University Paris-Sud, 91405 Orsay, France. Email: federica.agostini@u-psud.fr

†Department of Chemistry, Durham University, South Road, Durham DH1 3LE, United Kingdom. Email: basile.f.curchod@durham.ac.uk

Graphical Table of Contents

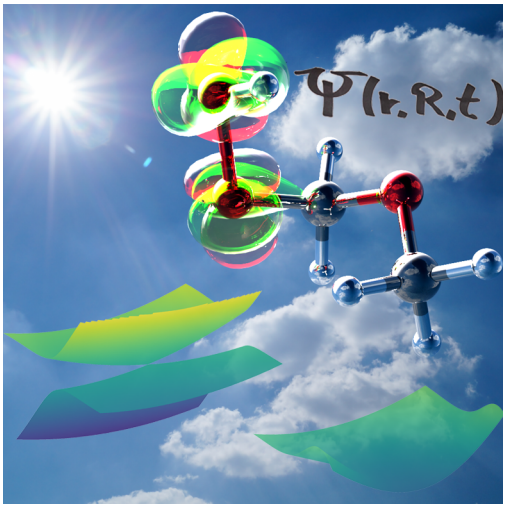

Contents

1 Introduction – Nonadiabatic dynamics

A set of moving nuclei, held together by electrons – this can summarize a common and simple depiction of a molecule. This vision, however, indirectly implies that nuclear motion can be somehow separated from the electronic one, and that electrons quantum-mechanically glue the nuclei in a specific way. Both are direct consequences of invoking the so-called Born-Oppenheimer approximation (BOA). Massively successful when used to investigate the vast majority of chemical reactivity (from reaction mechanisms to molecular properties), the BOA has forged our vision of molecules [1].

But a molecule should in principle be considered as a fully quantum object, with its quantum state defined by a molecular wavefunction. What the Born-Oppenheimer picture allows us to do is to reduce the complexity of this molecular wavefunction, by considering only the lowest-energy way of gluing the nuclei of a molecule together. More precisely, a molecule can be depicted, within the BOA, by a single nuclear wavefunction, whose dynamics is dictated by a single electronic eigenstate (often the lowest in energy, the ground electronic state). Hence, the BOA permits to neglect the fact that the motion of the nuclei can trigger a change in electronic eigenstate – we can consider that the nuclei evolve *adiabatically* in the ground electronic state, that is, without the possibility for the nuclei to give energy to the electrons to trigger an electronic transition. The reason for the success of the BOA when applied to ground-state chemistry becomes clear: at room temperature, it is rather unlikely (even if not impossible) that the motion of the nuclei is energetic enough to promote electrons from one eigenstate to another, as several electron volts separate electronic eigenstates (and 1 electron volt is worth 11'600 K of thermal energy). Within this framework, replacing the dynamics of a nuclear wavefunction by the one of classical particles would eventually bring us to an ever simpler depiction of a molecule, that of classical nuclei held together by an electronic cloud.

When, and how, is this picture offered by the BOA likely to break down? When the motion of the nuclei can trigger an electronic transition! The simplest case is when electronic eigenstates are close in energy. For example, the excited-state nuclear dynamics of a molecule, following its photoexcitation by light, is very likely to reach regions of the nu-

clear configuration space where electronic states become close in energy, allowing electronic transitions to take place mediated by nuclear motion: a *nonadiabatic* process [1]. Describing nonadiabatic processes in molecules forces us to step back and to reconsider our representation of the molecular wavefunction, accounting for the intricate coupling between nuclear and electronic motion. Nuclear quantum effects are likely to play an important role too, as nuclei can end up in a superposition of electronic states following a nonadiabatic event.

We propose here an Overview of the different strategies to simulate the dynamics of molecules beyond the BOA, with a clear focus on the description of nonadiabatic processes during the excited-state dynamics. As a starting point, we propose to visualize the time-dependent molecular wavefunction for a simple system, when the BOA is valid, and when it breaks down. Then, we will use this initial discussion to introduce two representations of the molecular wavefunction, Born-Huang and the Exact Factorization, and will highlight how each representation depicts the nonadiabatic dynamics of a molecule. A discussion follows on a selection of successful strategies to simulate the excited-state dynamics of molecules. We conclude by some outlooks of current developments in the field.

2 Stating the problem – the time-dependent molecular wavefunction

In a quantum picture, the behavior of a molecule is described by its time-dependent molecular wavefunction $\Psi(\mathbf{r}, \mathbf{R}, t)$. In this notation, $\mathbf{r}$ and $\mathbf{R}$ are vectors of electronic and nuclear coordinates, respectively. Hence, $\Psi(\mathbf{r}, \mathbf{R}, t)$ is a complicated object encoding the coupled dynamics of the electrons and nuclei. In a non-relativistic framework, the dynamics of the molecular wavefunction is dictated by the time-dependent Schödinger equation,

$$i\hbar\frac{\partial}{\partial t}\Psi(\mathbf{r}, \mathbf{R}, t) = \hat{H}(\mathbf{r}, \mathbf{R})\Psi(\mathbf{r}, \mathbf{R}, t)\,. \tag{1}$$

$\hat{H}(\mathbf{r}, \mathbf{R})$ is the molecular Hamiltonian and will be described in more details later (see Eq. (2)).

[1] The breakdown of the BOA is not restricted to nonadiabatic processes, and some chemical reactions in the ground electronic state can necessitate a more accurate description of the coupled electron-nuclear dynamics (see for example Refs. [2, 3, 4]).

As $\Psi(\mathbf{r}, \mathbf{R}, t)$ is the central quantity from which the different strategies for nonadiabatic dynamics will branch, one shall probably start this Overview by asking ourselves the question: *how does this molecular wavefunction look like?* The high dimensionality of $\Psi(\mathbf{r}, \mathbf{R}, t)$ makes it usually hard to visualize, but one can use here a simple molecular model of a coupled proton-electron transfer reaction to understand the main features of the molecular wavefunction [5]. In this one-dimensional model, depicted in Fig. 1, a proton (red circle) and an electron (gray cloud) move between two fixed positive charges (gray circles, separated by a distance L), and artificially altering the interaction between these two moving particles allows us to generate different physical conditions. For this one-dimensional system, the molecular wavefunction becomes $\Psi(r, R, t)$, where r is the position of the electron with respect to the center between the two fixed charges ('0' in Fig. 1), and R is the one of the moving proton.

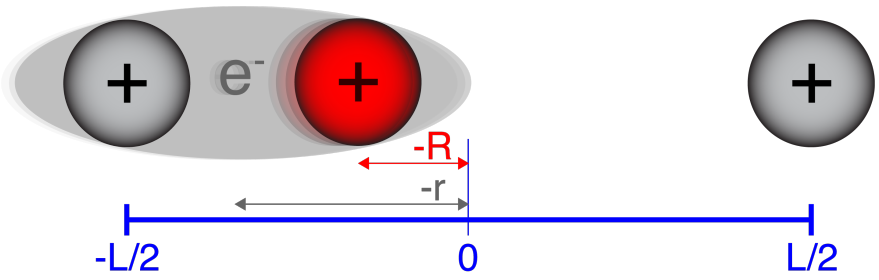

Figure 1: Schematic representation of a one-dimensional model for a coupled proton-electron transfer reaction. Two positive charges are fixed (grey) at a position $R_{\text{fixed},1} = -10$ bohr and $R_{\text{fixed},2} = 10$ bohr, giving a fixed distance L = 20 bohr. A moving proton (red circle) and electron (e^-) can evolve along the axis defined by the two fixed charges. Their respective position is characterized by R (proton) and r (electron). This model is strictly one-dimensional.

The time-dependent Schrödinger equation can be solved exactly for this model, and we propose here to study what happens quantum-mechanically when the proton, originally located in the vicinity of the left fixed charge (negative R), is kicked towards the fixed charge on the right (positive R)[2]. To highlight the appearance of nonadiabatic effects, this dynamics

[2]The initial molecular wavefunction $\Psi(r, R, t_0)$ is given by the product of a Gaussian nuclear wavepacket

will be performed for two cases: (a) the proton and the electron interact *strongly* and (b) the interaction between the proton and the electron is artificially diminished[3].

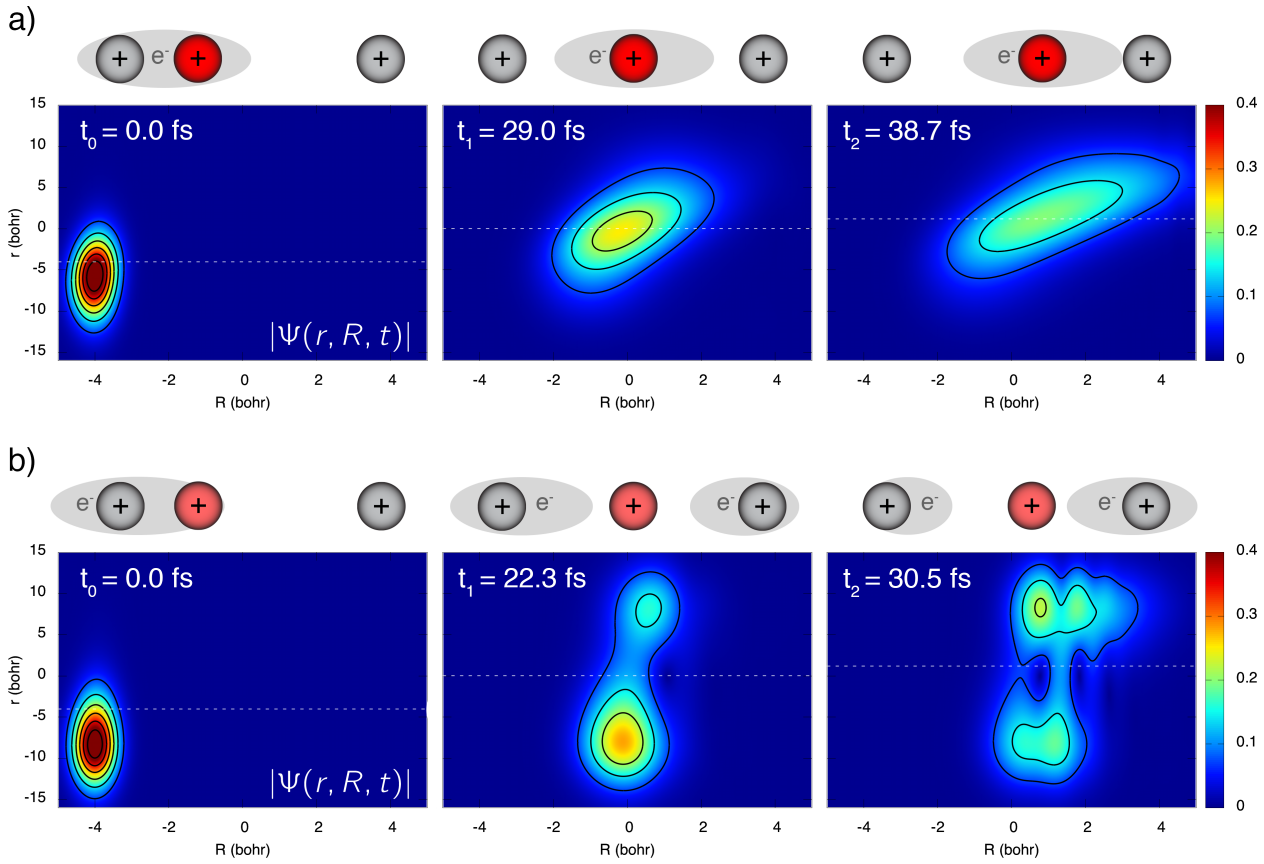

Figure 2: Snapshots of the modulus of the total molecular wavefunction, $|\Psi(r, R, t)|$, at three different times during the quantum molecular dynamics of the coupled electron-proton transfer model. The upper and lower panel give the snapshots for two different dynamics: dynamics with a strong (a) or a weak (b) interaction between the moving proton and electron. The top of each panel proposes a schematic representation of the studied dynamics. The white horizontal dashed line gives the expectation value of the position of the moving proton.

(multiplied by a phase factor accounting for a non-zero initial average value of the nuclear momentum operator) with the electronic ground eigenfunction of the model system.

[3]It is important to note that by modifying the interaction between the moving proton and the electron one alters the electronic structure of the problem, and therefore the likelihood of nonadiabatic processes. This is not the only way to enhance the nonadiabatic character of the dynamics for this model system. Another strategy would have consisted in varying the initial momentum of the moving proton. For the proposed system, larger momenta would lead to higher probabilities for nonadiabatic transitions.

The upper panel of Figure 2 shows three snapshots of the total molecular wavefunction modulus ($|\Psi(r, R, t)|$) for the dynamics in case (a), that is, when the interaction between the electron and the proton is strong. In this representation, the nuclear coordinate R follows the x-axis, while the y-axis is used for the electronic coordinate r. At the beginning of the dynamics (t_0), the proton (R) is centered at $R = -4$ bohr, close to the left fixed charge. The electron (r) is located between the fixed charge centered at $R_{\text{fixed},1} = -10$ bohr and the moving proton (note the larger delocalization of the light electron as compared to the heavier proton). At a later time (t_1), the proton is at an equal distance between the two fixed charges ($R = 0$ bohr) and is more spread than at the initial time. More importantly, one can observe that the electron closely follows the moving proton: the electron is centered around the expectation value of the nuclear position, symbolized by a horizontal white dashed line in Fig. 2a. The proton continues its journey towards the other fixed charge (t_2), always closely followed by the electron. A schematic representation for each time snapshot is provided on top of the corresponding graphic to better illustrate the dynamics of the total system. To summarize, the situation (a) leads to a coupled electron-nuclear dynamics where the electron follows the moving proton. In other words, the electron instantaneously adapts to the nuclear dynamics – a situation reminiscent to what motivates the BOA.

The situation differs dramatically when the interaction between the electron and the proton is weakened (Fig. 2, panel b). At t_0, the proton is at the same position as in case (a), but the electron is now more localized around the left fixed charge (centered at -10 bohr) due to the weaker interaction with the moving proton. The electron does not follow the moving proton closely anymore when it departs from the negative R region (t_1): it becomes delocalized around both fixed charges. This process, which can be ascribed to an electron transfer from the left fixed charge to the right one, is further amplified at later times (t_2), when the proton enters the positive-R region. Hence, the dynamics of the proton triggers a substantial change in the electronic configuration of the system. This Overview will focus on such phenomena, when a strong interplay between nuclear and electronic dynamics takes place in a molecule.

The representation of the full molecular wavefunction is in general impractical for larger molecular systems. Also, the coupled electron-nuclear dynamics presented above, and the

complexity of Fig. 2, makes it clear that a strategy is required to better *represent* the molecular wavefunction – 'better' meaning here that the representation should provide a different, possibly simpler, understanding of the interplay between nuclear and electronic dynamics. In the following Sections, we will introduce two different *representations* for $\Psi(\mathbf{r}, \mathbf{R}, t)$ and discuss how the dynamics of the coupled proton-electron transfer model can be translated in the eyes of each of these representations.

3 Nonadiabatic Dynamics – the Born-Huang perspective

3.1 Theoretical formalism

The Hamiltonian $\hat{H}(\mathbf{r}, \mathbf{R})$ of a molecular system, encountered earlier in the molecular Schrödinger equation (Eq. (1)), is given by

$$\begin{aligned}\hat{H}(\mathbf{r}, \mathbf{R}) &= \sum_{\nu=1}^{N_n} \frac{-\hbar^2}{2M_\nu} \nabla_\nu^2 + \hat{T}_e(\mathbf{r}) + V_{ee}(\mathbf{r}) + V_{nn}(\mathbf{R}) + V_{en}(\mathbf{r}, \mathbf{R}) \\ &= \sum_{\nu=1}^{N_n} \frac{-\hbar^2}{2M_\nu} \nabla_\nu^2 + \hat{H}_{BO}(\mathbf{r}, \mathbf{R}) \,. \end{aligned} \tag{2}$$

The first term on the right-hand side is the nuclear kinetic energy, with $\nabla_\nu = \frac{\partial}{\partial \mathbf{R}_\nu}$ indicating the spatial derivative with respect to the position of the nucleus ν (with mass M_ν). $\hat{H}_{BO}(\mathbf{r}, \mathbf{R})$ is the Born-Oppenheimer (BO) Hamiltonian, sometimes also called electronic Hamiltonian. $\hat{H}_{BO}(\mathbf{r}, \mathbf{R})$ is defined as the sum of the electronic kinetic energy ($\hat{T}_e$), the electron-electron ($\hat{V}_{ee}$), the nucleus-nucleus (V_{nn}), and the electron-nucleus (V_{en}) interactions.

Fixing the nuclei at a given nuclear configuration (or assuming that they have an infinite mass) [6, 1, 7] sets the nuclear kinetic energy to zero, and the time-independent Schrödinger equation for the $\hat{H}_{BO}(\mathbf{r}, \mathbf{R})$ Hamiltonian at this nuclear configuration can be solved:

$$\hat{H}_{BO}(\mathbf{r}, \mathbf{R}) \varphi_{\mathbf{R}}^{(l)}(\mathbf{r}) = \epsilon_{BO}^{(l)}(\mathbf{R}) \varphi_{\mathbf{R}}^{(l)}(\mathbf{r}) \,. \tag{3}$$

Eq. (3) is referred to as the time-independent *electronic* Schrödinger equation. Its eigenfunctions $\varphi_{\mathbf{R}}^{(l)}(\mathbf{r})$ are called *electronic wavefunctions* and depend parametrically on the nuclear configuration $\mathbf{R}$ (indicated as a subscript). An eigenvalue of Eq. (3), $\epsilon_{BO}^{(l)}(\mathbf{R})$, corresponds to

the *electronic energy* of the molecule in the electronic state l at a nuclear configuration $\mathbf{R}$, in the so-called *adiabatic representation*. Note that the electronic energy $\epsilon_{BO}^{(l)}(\mathbf{R})$, despite its name, also includes the nucleus-nucleus interaction potential $V_{nn}(\mathbf{R})$. If we compute these electronic energies for a large number of different nuclear configurations, we can reconstruct the potential energy surfaces (PESs) of a molecule.

Solving Eq. (3) gives access to a complete set of orthonormal electronic eigenfunctions. The central idea of the Born-Huang representation [8] is to use these eigenfunctions as a basis to express the time-dependent molecular wavefunction:

$$\Psi(\mathbf{r},\mathbf{R},t) = \sum_l \chi_{BO}^{(l)}(\mathbf{R},t)\varphi_{\mathbf{R}}^{(l)}(\mathbf{r})\,. \tag{4}$$

In Eq. (4), the $\chi_{BO}^{(l)}(\mathbf{R},t)$ are time-dependent and $\mathbf{R}$-dependent expansion coefficients, linked to the time-dependent nuclear density by $|\chi(\mathbf{R},t)|^2 = \sum_l |\chi_{BO}^{(l)}(\mathbf{R},t)|^2$ – as a result they are often called *nuclear amplitudes* or *nuclear wavefunctions*.

The total molecular Schrödinger equation can be rewritten within the Born-Huang representation by (*i*) inserting Eq. (4) into the time-dependent molecular Schrödinger equation Eq. (1), (*ii*) left-multiplying the result by $\varphi_{\mathbf{R}}^{(k)*}(\mathbf{r})$, and (*iii*) integrating over $\mathbf{r}$ (symbolized by $\langle\cdots\rangle_{\mathbf{r}}$). The resulting set of equations of motion for the nuclear amplitude (one per electronic state) reads

$$i\hbar\frac{\partial}{\partial t}\chi_{BO}^{(k)}(\mathbf{R},t) = \left[\sum_\nu^{N_n}\frac{-\hbar^2}{2M_\nu}\nabla_\nu^2 + \epsilon_{BO}^{(k)}(\mathbf{R})\right]\chi_{BO}^{(k)}(\mathbf{R},t) + \sum_l \mathcal{F}_{kl}(\mathbf{R})\chi_{BO}^{(l)}(\mathbf{R},t)\,. \tag{5}$$

The two terms in the square bracket are simply the nuclear kinetic energy and the electronic potential term. The Born-Huang representation leads to the following picture of the coupled electron-nuclear dynamics of a molecule: the electrons provide a time-independent PES on which a nuclear amplitude can evolve. There is one time-dependent amplitude per electronic state k, with corresponding PES $\epsilon_{BO}^{(k)}(\mathbf{R})$. But there is more: the last terms in Eq. (5), $\mathcal{F}_{kl}(\mathbf{R})$, connect nuclear amplitudes between different electronic states. $\mathcal{F}_{kl}(\mathbf{R})$ includes couplings between nuclear motion and electronic states, originating from the action of the nuclear kinetic energy operator on the electronic wavefunctions:

$$\mathcal{F}_{kl}(\mathbf{R}) = -\sum_\nu^{N_n}\frac{\hbar^2}{2M_\nu}\langle\varphi_{\mathbf{R}}^{(k)}|\nabla_\nu^2|\varphi_{\mathbf{R}}^{(l)}\rangle_{\mathbf{r}} - \sum_\nu^{N_n}\frac{\hbar^2}{M_\nu}\langle\varphi_{\mathbf{R}}^{(k)}|\nabla_\nu|\varphi_{\mathbf{R}}^{(l)}\rangle_{\mathbf{r}}\cdot\nabla_\nu\,. \tag{6}$$

The *first-order nonadiabatic coupling vectors*, $\mathbf{d}_{kl}(\mathbf{R}) = \langle\varphi^{(k)}_{\mathbf{R}}|\nabla_{\mathbf{R}}|\varphi^{(l)}_{\mathbf{R}}\rangle_{\mathbf{r}}$ (for $k \neq l$), and *second-order nonadiabatic couplings*, $D_{kl}(\mathbf{R}) = \langle\varphi^{(k)}_{\mathbf{R}}|\nabla^2_{\mathbf{R}}|\varphi^{(l)}_{\mathbf{R}}\rangle_{\mathbf{r}}$ ($\forall k, l$), bring all the nonadiabatic effects in the molecular dynamics, *i.e.*, they are responsible for the transfer of nuclear amplitude between different electronic states.

Setting all the $\mathcal{F}_{kl}(\mathbf{R})$ with $k \neq l$ to zero in Eq. (5) results in a dynamics where the nuclear amplitude is constrained to a single electronic eigenstate k. This approximation is known as the *BOA*, and corresponds to a full molecular wavefunction approximated by $\Psi(\mathbf{r}, \mathbf{R}, t) \approx \chi^{(k)}_{BO}(\mathbf{R}, t)\varphi^{(k)}_{\mathbf{R}}(\mathbf{r})$. Neglecting *all* the $\mathcal{F}_{kl}(\mathbf{R})$ in Eq. (5) is often referred to as the *adiabatic* BOA and is perhaps the most commonly employed version of this approximation [9].

3.2 Dynamics of the total molecular wavefunction in a Born-Huang picture

How does the dynamics of our coupled proton-electron transfer model look like in a Born-Huang picture? The first step consists in obtaining for this model the electronic energies for all possible nuclear configurations, forming the potential energy curve (PEC) $\epsilon^{(k)}_{BO}(R)$ for each electronic state considered (upper panels of Fig. 3). In the case (a), the two electronic states remain well separated over the entire range of R considered. Conversely, the energy of the ground and first electronic states are coming closer in the case (b). The electronic wavefunctions for both electronic states, $\varphi^{(S_0)}_R(r)$ and $\varphi^{(S_1)}_R(r)$, can also be represented as a function of R (lower panels of Fig. 3). It is important to stress here that these electronic wavefunctions are time-independent and that only the nuclear amplitudes have an explicit time dependence. In case (a), the ground-state electronic wavefunction has its maximum smoothly switching from the negative to the positive r-region as the value of R changes from negative to positive. The corresponding S_1 wavefunction shows the same trend as the one of S_0, but with the addition of a nodal line. The S_0 and S_1 electronic wavefunctions in the case (b) exhibit a very different behavior. In S_0, the electronic wavefunction remains mostly located around the left fixed charged for any negative R, and abruptly changes localization for positive R, being now centred around the right fixed charge. The S_1 wavefunction, in the range $-4 < R < 4$ bohr, is a mirror image of the S_0 wavefunction: the electronic

wavefunction in this first excited state is located around the right fixed charge at negative R and around the left fixed charge for positive R. An electronic excitation from S_0 to S_1 at negative R would correspond to an electron transfer from the left fixed charge to the right one. We note that for $R < -4$ bohr and $R > 4$ bohr, the electronic wavefunction changes character and resembles more the one observed in case (a). Hence, the electronic eigenfunctions and eigenvalues clearly translate the difference in electron-proton interaction between the case (a) and (b).

Let us now focus on the nuclear dynamics resulting from the solution of Eqs. (5) (upper panels of Fig. 3). The Born-Huang picture describes the initial state (defined above) as a nuclear wavefunction $\chi_{BO}^{(S_0)}(R, t_0)$ localized at $R = -4$ bohr in S_0 (blue curve, upper panel of Fig. 3a), which evolves on the PEC $\epsilon_{BO}^{(S_0)}(R)$. The initial wavefunction is given a small positive momentum to trigger the dynamics of the proton from the left fixed charge towards the right one.

For case (a), where the moving proton has a strong interaction with the electron (upper panel of Fig. 3a), the nuclear wavefunction simply travels along the S_0 PEC, with no amplitude transfer to S_1. Hence, the Born-Huang representation shows that the nuclear dynamics solely takes place on $\epsilon_{BO}^{(S_0)}(R)$ without nonadiabatic effects: the electron closely follows the moving proton, and case (a) is a perfect example of a molecular quantum dynamics for which the BOA is fully valid. One can rationalize this adiabatic dynamics by the large energy gap between S_0 and the other electronic states. As the nonadiabatic coupling vectors are inversely proportional to the energy gap between the two electronic states considered, all terms $\mathcal{F}_{S_0 l}(R)$ in Eq. (5) are negligible in the case (a).

The picture becomes substantially more complex for the case (b). The initial state at time t_0 is the same as for (a). However, a transfer of nuclear amplitude takes place between S_0 and S_1 by the time t_1 (Fig. 3b, plain and dotted orange lines, respectively), when the moving charge reaches $R = 0$ bohr. The electronic character of the molecular system can be analyzed in terms of its contributions from S_0 and S_1, based on the region where the nuclear amplitude is localized: (i) the nuclear wavefunction in S_0 is centered around $R = 0$, thus the electronic localization switches abruptly from the left fixed charge (for $R < 0$) to the right one (for $R > 0$); (ii) the nuclear contribution in S_1 is more on the positive R side, thus

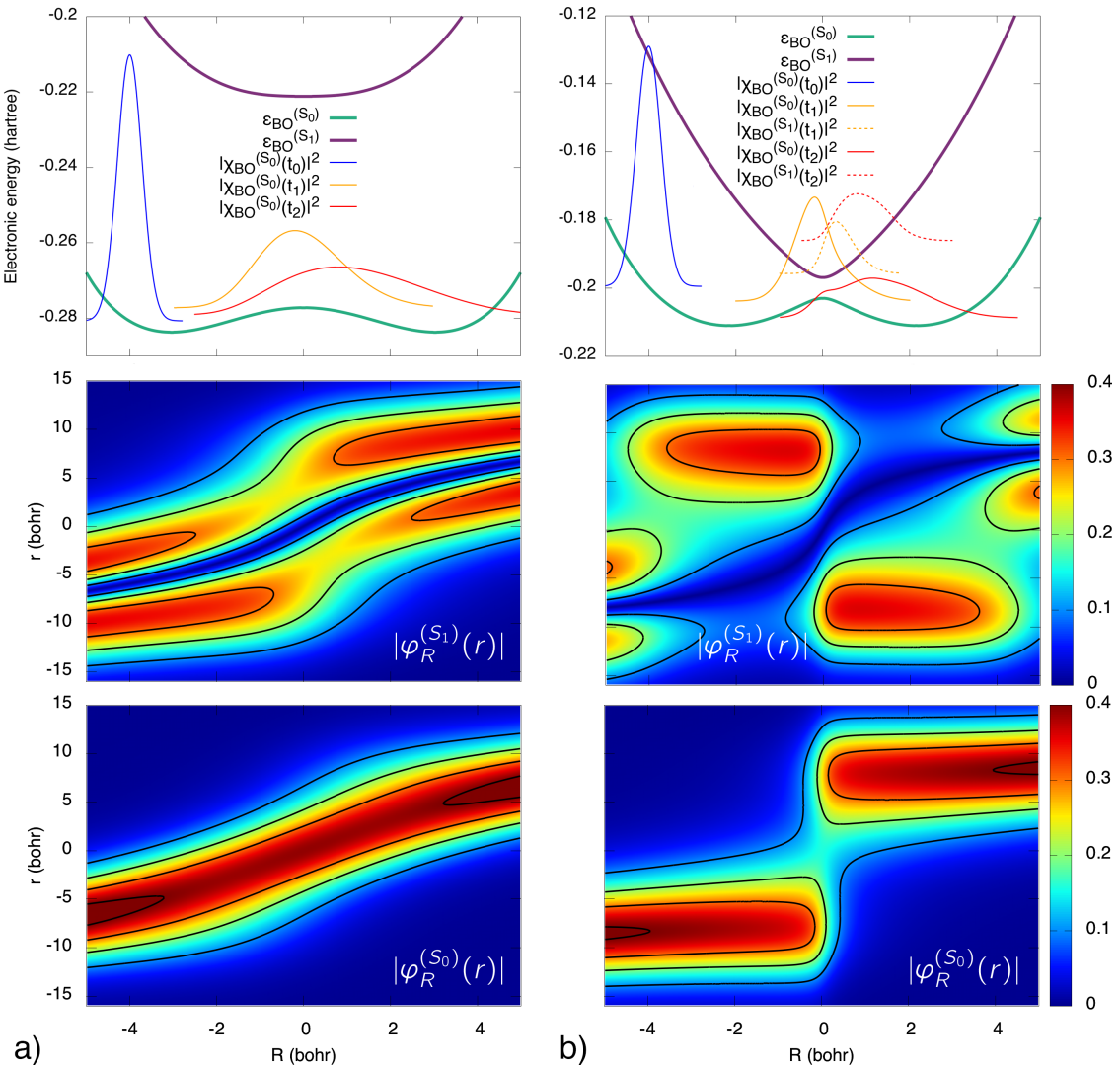

Figure 3: Born-Huang representation of the molecular quantum dynamics described in Fig. 2, for the two cases (a) and (b). Upper panels show the PECs, as well as the squared-modulus of the time-dependent nuclear amplitudes at the three different times t_0 (blue), t_1 (orange), and t_2 (red). The middle and lower panels corresponds to the the modulus of the S_1 and S_0 time-independent electronic wavefunctions, respectively.

the electron is mainly localized around the left fixed charge. Hence, at time t_1, the moving proton is mostly around $R = 0$, while the electron is delocalized both around the left and the right fixed charge, with more amplitude around the left one – as depicted by the molecular wavefunction in the second panel of Fig. 2b. At time t_2, the nuclear amplitudes in S_0 and S_1 are both on the positive R side, implying that the electron is still delocalized around the

two fixed charges. The molecular quantum dynamics in case (b) is highly nonadiabatic as the nuclear dynamics does not follow a single electronic eigenstate and the coupling between electronic and nuclear motion induces nuclear amplitude transfer between electronic states.

We should note, at this stage, that the concepts used in this paragraph are those employed commonly to describe photochemical and photophysical processes, and therefore our understanding of these phenomena is deeply rooted in the Born-Huang representation: one often thinks about excited-state molecular processes in terms of a molecule transferring between coupled PESs during nonradiative relaxation processes.

4 Nonadiabatic Dynamics – the Exact-Factorization perspective

4.1 Theoretical formalism

The solution of the time-dependent Schrödinger equation (1) can always be written as the product [10, 11, 12]

$$\Psi(\mathbf{r},\mathbf{R},t) = \chi(\mathbf{R},t)\Phi_{\mathbf{R}}(\mathbf{r},t). \tag{7}$$

The time-dependent functions $\chi(\mathbf{R},t)$ and $\Phi_{\mathbf{R}}(\mathbf{r},t)$ are the nuclear wavefunction and the conditional electronic wavefunction, respectively. The conditional electronic wavefunction depends parametrically on the nuclear configuration, very much like the time-independent electronic wavefunctions introduced earlier. This Exact-Factorization idea is the time-dependent generalization of earlier work [13, 14, 15, 16, 17], and extends the product form of the stationary joint probability $|\Psi(\mathbf{r},\mathbf{R})|^2$ into marginal and conditional probabilities $|\chi(\mathbf{R})|^2|\Phi_{\mathbf{R}}(\mathbf{r})|^2$ to the probability amplitudes $\Psi(\mathbf{r},\mathbf{R}) = \chi(\mathbf{R})\Phi_{\mathbf{R}}(\mathbf{r})$. The interpretation of $\Phi_{\mathbf{R}}(\mathbf{r},t)$ as a time-dependent conditional probability amplitude requires to impose a partial normalization condition $\int d\mathbf{r}|\Phi_{\mathbf{R}}(\mathbf{r},t)|^2 = 1\ \forall\,\mathbf{R},t$.

The time evolution of $\Psi(\mathbf{r},\mathbf{R},t)$ is dictated by the time-dependent Schrödinger equation with Hamiltonian (2). Therefore, the nuclear and conditional electronic wavefunctions evolve

according to the equations

$$i\hbar\frac{\partial}{\partial t}\chi(\mathbf{R},t) = \left[\sum_{\nu}^{N_n}\frac{\left[-i\hbar\nabla_\nu + \mathbf{A}_\nu(\mathbf{R},t)\right]^2}{2M_\nu} + \epsilon(\mathbf{R},t)\right]\chi(\mathbf{R},t) \tag{8}$$

$$i\hbar\frac{\partial}{\partial t}\Phi_{\mathbf{R}}(\mathbf{r},t) = \left[\hat{H}_{BO}(\mathbf{r},\mathbf{R}) + \hat{U}_{en}[\Phi_{\mathbf{R}},\chi] - \epsilon(\mathbf{R},t)\right]\Phi_{\mathbf{R}}(\mathbf{r},t)\,, \tag{9}$$

which are derived [18] by inserting the product form of the molecular wavefunction into the time-dependent Schrödinger equation and imposing the normalization condition on $\Phi_{\mathbf{R}}(\mathbf{r},t)$. Eq. (8) is a time-dependent Schrödinger equation with nuclear Hamiltonian defined in square brackets. Here, the time-dependent vector potential $\mathbf{A}_\nu(\mathbf{R},t) = \langle\Phi_{\mathbf{R}}(t)| - i\hbar\nabla_\nu\Phi_{\mathbf{R}}(t)\rangle_{\mathbf{r}}$ and time-dependent potential energy surface (TDPES) $\epsilon(\mathbf{R},t) = \langle\Phi_{\mathbf{R}}(t)|\hat{H}_{BO}+\hat{U}_{en}-i\hbar\frac{\partial}{\partial t}|\Phi_{\mathbf{R}}(t)\rangle_{\mathbf{r}}$ express the coupling of nuclear and electronic motion[4]. Eq. (9) yields the evolution of the electronic wavefunction, where the coupling to the nuclear dynamics is encoded in the electron-nuclear coupling operator $\hat{U}_{en} = \sum_\nu \frac{1}{M_\nu}\big[\frac{[-i\hbar\nabla_\nu - \mathbf{A}(\mathbf{R},t)]^2}{2} + (\frac{-i\hbar\nabla_\nu\chi(\mathbf{R},t)}{\chi(\mathbf{R},t)} + \mathbf{A}(\mathbf{R},t))\cdot(-i\hbar\nabla_\nu - \mathbf{A}(\mathbf{R},t))\big]$. Since $\hat{U}_{en}$ acts on the parametric dependence of the electronic wavefunction, and the vector potential and TDPES depend on $\Phi_{\mathbf{R}}(\mathbf{r},t)$, Eq. (9) is not a Schrödinger equation and is non-linear.

The product in Eq. (7) is invariant upon multiplication of $\Phi_{\mathbf{R}}(\mathbf{r},t)$ by a $\mathbf{R},t$-dependent phase factor and $\chi(\mathbf{R},t)$ by its complex conjugate. Hence, the factorization appears as not uniquely defined. However, this is the only freedom in the definition of $\chi(\mathbf{R},t)$ and $\Phi_{\mathbf{R}}(\mathbf{r},t)$, if the partial normalization condition is imposed, and uniqueness can be ensured upon *fixing the gauge*: once the $\mathbf{R},t$-dependent phase factor is chosen, the wavefunctions at all times are uniquely determined by Eqs. (8) and (9). The choice of gauge does not affect either the form of the evolution equations or the observables.

4.2 The Exact Factorization 'beyond the equations'

What interpretation of the coupled electron-nuclear dynamics of a molecule results from the Exact Factorization? This representation seems to complicate the problem by translating the time-dependent Schrödinger equation into two coupled partial differential equations, one

[4]Even though $\hat{U}_{en}$ depends on χ, this dependence disappears in $\langle\Phi_{\mathbf{R}}(t)|\hat{U}_{en}|\Phi_{\mathbf{R}}(t)\rangle_{\mathbf{r}}$. Therefore, the nuclear Hamiltonian does not depend on χ.

of which is non-linear. So, why should one be interested in the Exact Factorization?

First of all, the Exact Factorization represents nuclear dynamics in terms of a nuclear wavefunction propagating under the effect of a *single* driving potential *independently* of the adiabatic or nonadiabatic character of the problem. The potential is time-dependent and expressed in the form of a vector-potential and a scalar-potential (the TDPES) contribution in the nuclear time-dependent Schrödinger equation (8). Why is this important? Having a single potential allows one to uniquely introduce the concept of a *classical force*, that can be used in an approximate form of the nuclear evolution equation, for instance by using classical-like trajectories. Conversely, the Born-Huang framework invokes *multiple* static electronic PESs driving the motion of nuclear amplitudes and nonadiabatic couplings inducing amplitude transfers between states. A single potential is recovered only within the BOA. Therefore, Born-Oppenheimer molecular dynamics can be performed by simply computing the force from the PES that corresponds to the single electronic state populated during the whole dynamics. This simple picture is lost in nonadiabatic situations within the Born-Huang framework.

Second, the electronic dynamics is expressed in a *representation-free* form. While the Born-Huang framework relies on a basis expansion, the Exact Factorization is merely a rewriting of the Schrödinger equation for the molecular wavefunction. Conceptual and/or numerical issues related to the definition of the electronic basis set chosen for the expansion are naturally circumvented. In particular, this feature allows one to rethink molecular dynamics at conical intersections [19, 20] and phenomena related to geometric phases [21], which can be grounded in the Born-Huang representation and sometimes (mis-)interpreted as observable effects. Despite this intriguing possibility, practical numerical applications of the Exact Factorization (see Section 5.1.2 and Refs. [22, 23, 24]) still rely on a Born-Huang-like expansion of the electronic wavefunction, in order to employ standard quantum-chemistry approaches to compute electronic properties along the nuclear dynamics. A question arises, as to whether one can employ the *representation-free* nature of the Exact Factorization for excited-state molecular dynamics without the support of quantum-chemistry calculations to determine electronic-structure properties. Recent works [25, 26] have set the first basis for such a developments.

4.3 Dynamics of the total molecular wavefunction in the Exact-Factorization picture

We analyze here how the Exact Factorization depicts the dynamics of our coupled proton-electron transfer model discussed in previous Sections[5]. As this particular example is one-dimensional in the nuclear configuration space, the gauge can be chosen such that the time-dependent vector potential is identically zero (see Ref. [27] for the details of this procedure). While this choice of gauge cannot be generalized to higher dimensions, it allows for a simple identification of the key features of the Exact Factorization.

In case (a), where the electron and moving ion are strongly interacting, the dynamics described by the Exact Factorization is the same as in the Born-Huang picture: at time t_0 the nuclear density is localized around the position $R = -4$ bohr and has a Gaussian shape; at time t_1 the density broadens while crossing the maximum of the S_0 PEC; at time t_2 the nuclear density is mainly located in the positive R region, even more delocalized. We point out that there is no difference between the Born-Huang and the Exact-Factorization nuclear density, because the latter, thanks to the partial normalization condition on the conditional electronic wavefunction, yields the exact nuclear many-body density as $|\chi(R,t)|^2$.

Let us now focus on what drives the nuclear dynamics: the time-dependent potential energy curve (TDPEC) $\epsilon(R,t)$ (upper panel of Fig. 4a and 4b). In the following, we focus on the so-called gauge-independent (GI) contribution to the TDPEC, $\epsilon_{GI}(R,t)$, as it exhibits some specific features connecting to our earlier discussion on the Born-Huang representation. The second contribution to the TDPEC is gauge-dependent ($\epsilon_{GD}(R,t)$). In case (a) $\epsilon_{GD}(R,t)$ is just a constant function of R, while in case (b) it is either constant or stepwise constant with steps appearing at the same positions as the steps in $\epsilon_{GI}(R,t)$ but with opposite sign. The interested reader is referred to Refs. [28, 27] for more information on these two contributions to the TDPEC.

[5]In the following, the Exact-Factorization quantities are obtained from the numerically exact solution of the full time-dependent Schrödinger equation presented in Section 2. Based on this result, the time-dependent electronic and nuclear wavefunctions are computed from the resulting time-dependent molecular wavefunction and inserted into the expression for the TDPES (discussed in Section 4.1). For more information on the numerical procedure to compute Exact-Factorization quantities, the reader is referred to Ref. [27]

In the case (a), $\epsilon_{GI}(R,t)$ follows exactly the shape of the S_0 PEC, and it evolves from time t_0 to time t_2 only because it is calculated in the region of non-negligible nuclear density[6]. This result is somehow striking, because the time-dependent Schrödinger equation, or equivalently the Exact-Factorization equations (8) and (9), do not have any knowledge of the adiabatic PECs (or PESs) or the adiabatic states. Nevertheless, the ground-state PEC naturally emerges as the potential driving the nuclear dynamics in adiabatic conditions. The same observation can be applied to the conditional electronic wavefunction (lower panels of Fig. 4a). As for $\epsilon_{GI}(R,t)$, the quantity $|\Phi_R(r,t)|$ is shown only for the values of R where the nuclear density is non-zero. The Exact Factorization also represents the dynamics as purely adiabatic: no difference can be seen between $|\varphi_R^{(S_0)}(r)|$ in the lowest panel of Fig. 3a and the snapshots at times t_0 to t_2 of $|\Phi_R(r,t)|$ in Fig. 4a.

The nonadiabatic case (b) shows how the GI part of the TDPEC is capable of encoding different characters of the electronic wavefunction, and this information is translated here into a Born-Huang framework. $\epsilon_{GI}(R,t)$ is identical to the S_0 potential at time t_0 (blue curve, upper left panel of Fig. 4b): the nuclear wavefunction evolves initially under the effect of the ground-state potential. At time t_1, the shape of the GI-TDPEC (orange curve, upper center panel of Fig. 4b) deviates from a purely adiabatic shape: it follows S_0 for $R < 0$, but lies between S_0 and S_1 for $R > 0$. At time t_2, the GI-TDPEC (red curve, upper left panel of Fig. 4b) (*i*) smoothly connects S_0 to S_1 in the region around $R = 0$, (*ii*) is purely adiabatic for $R > 3$ bohr, and (*iii*) presents a smooth step in the region $1.5 < R < 3$ bohr, connecting the shapes of (*i*) and (*ii*). Let us analyze further the right panels in Fig. 4b. In the region $R > 3$ bohr, the nuclear dynamics is governed by S_0, and as shown in the Born-Huang formulation, the nuclear density contribution in this region arises only from the projection on S_0 (plain red curve, upper panel of Fig. 3b). In the step region ($1.5 < R < 3$ bohr), instead, the GI-TDPEC changes character, switching from S_1 to S_0. The question is then: can one observe such a switch of character in $\Phi_R(r,t_2)$? The answer is yes: in the region $1.5 < R < 3$ bohr, $|\Phi_R(r,t_2)|$ has maxima in both positive and negative regions of r. However, if one looks at the adiabatic states of Fig. 3b, $|\varphi_R^{(S_0)}(r)|$ is nearly zero in the region $R > 0, r < 0$, whereas$|\varphi_R^{(S_1)}(r)|$ has a non-zero contribution.

[6]This limitation is only due to numerical reasons, as the TDPEC is defined everywhere in space.

The opposite situation can be observed for $R > 0, r > 0$. The conclusion is that the GI-TDPEC, for $1.5 < R < 3$ bohr, switches from the ground to the excited PEC because the character of $\Phi_R(r, \mathrm{t}_2)$ mimics a change from the ground to the excited adiabatic state. However, this is not always true, because at t_0 $|\Phi_R(r, \mathrm{t}_0)| \simeq |\varphi_R^{(S_0)}(r)|$ is purely adiabatic. The time dependence of the potential that drives the nuclear dynamics is clearly essential to encode all changes in the character of the conditional electronic wavefunction over time. Conversely, the Born-Huang representation pictures such changes of character as nuclear amplitude transfers among electronic adiabatic states.

Before concluding this Section, it is instructive to compare $|\Phi_R(r,t)|$ of Fig. 4 with $|\Psi(r,R,t)|$ of Fig. 2 in the r-direction. By virtue of the Exact Factorization Eq.(7), the conditional electronic wavefunction contains all the information about the dependence of the molecular wavefunction on the electronic coordinate. Therefore, it is easy to compare the two functions along the r-direction, and identify, for instance, the regions of larger probability of finding the electron: $|\Phi_R(r,t)|$ has clearly the same features as $|\Psi(r,R,t)|$, and this is evident at all times. In the Born-Huang framework, instead, the analysis of the adiabatic eigenfunctions $|\varphi_R^{(S_0)}(r)|$ and $|\varphi_R^{(S_1)}(r)|$ does not give access to this information in such a straightforward way.

5 Simulating the nonadiabatic dynamics of molecules

Even though being only one-dimensional, the model system and scheme introduced above highlight the different components introduced by a Born-Huang description of nonadiabatic phenomena and their complex interplay. In general, one needs to account (*i*) for more than one electronic state, (*ii*) for transfer of nuclear amplitude between electronic states, and (*iii*) for possible quantum-interference effects between the nuclear amplitudes on different states. Simulating the nonadiabatic dynamics of a molecular system can therefore be split into two different *contributions*: the *electronic-structure* contribution – how can I obtain $\epsilon_{BO}^{(k)}(\mathbf{R})$, $\mathbf{d}_{kl}(\mathbf{R})$, or $D_{kl}(\mathbf{R})$ for all the electronic states? – and the *nuclear dynamics* contribution – how shall I describe the nuclear dynamics, or, how can I approximate nuclear quantum effects? As this Overview intends to present an *aperçu* of the different strategies to perform

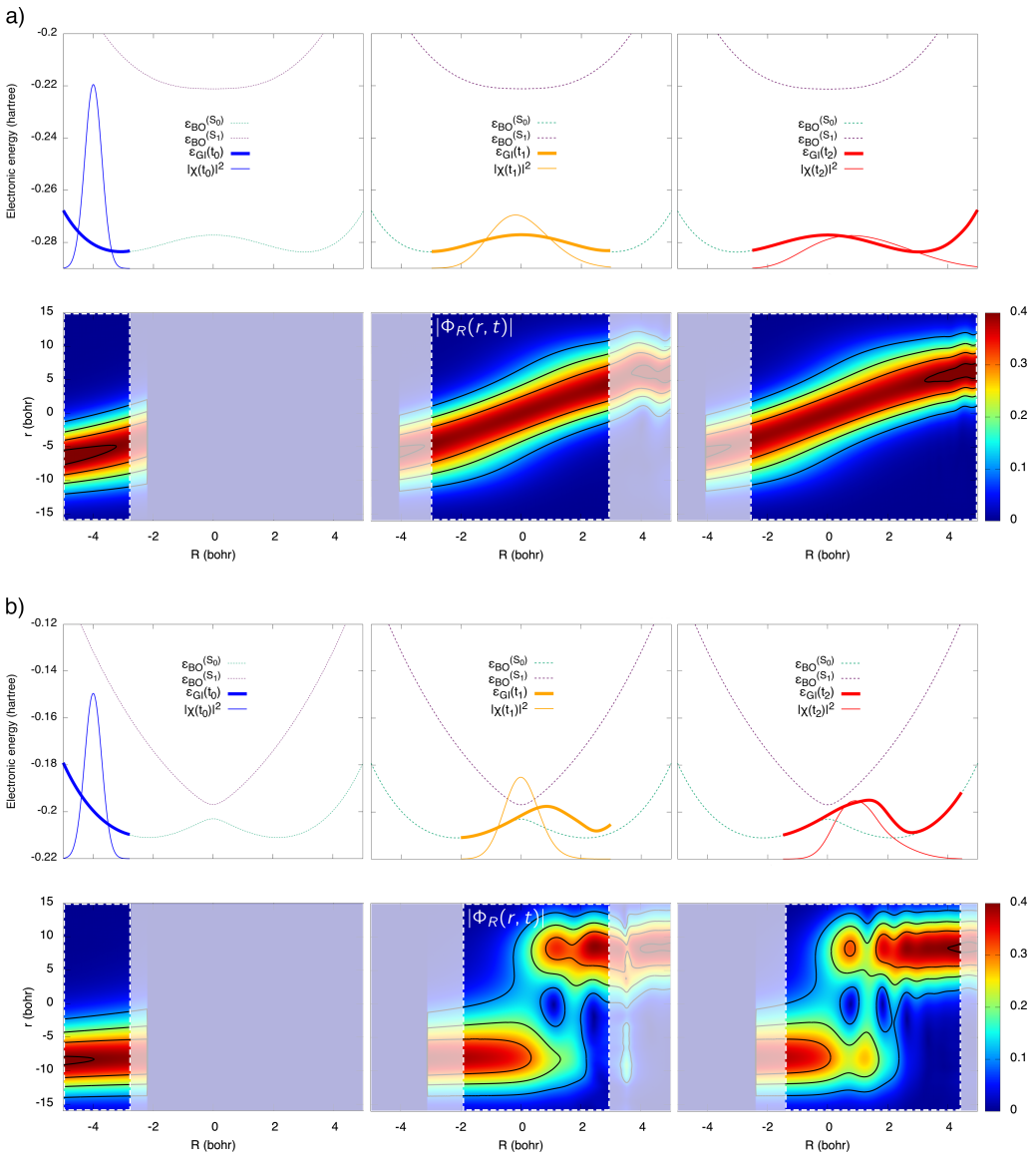

Figure 4: Exact-Factorization representation of the molecular quantum dynamics described in Fig. 2, for the two cases (a) and (b). For each case, the gauge-independent (GI) part of the TDPES ($\epsilon_{GI}(R,t)$) is plotted on the upper panels and compared to the PECs of the corresponding model, along with the nuclear density. From left to right, snapshots along the dynamics for times t_0 (blue curves), t_1 (orange curves), and t_2 (red curves) are shown. The modulus of the conditional electronic wavefunction is showed in the lower panels. The white dashed boxes highlight the regions of non-negligible nuclear amplitude, where the Exact-Factorization quantities are computed.

nonadiabatic dynamics on molecules, the following section will focus exclusively on the latter question related to nuclear dynamics. The use of electronic structure theory for excited electronic states is, for example, discussed in great detail in Refs. [29, 30, 31, 32, 33, 10, 34, 35, 36, 37]. Furthermore, we discuss here only a selected number of methods from this very fertile field of research, and further insights can be gained by consulting the referenced reviews and book chapters.

5.1 Different strategies for the nuclear dynamics

Armed with all the required electronic structure quantities, let us focus on the propagation of the nuclear amplitudes (in a Born-Huang framework, Eq. (5)) or of the nuclear wavefunction (in an Exact-Factorization framework, Eq. (8)). In the following, we highlight a selection of important strategies to perform nonadiabatic nuclear dynamics that have been applied to the study of molecular systems and range from highly-accurate grid-based techniques to more approximate – yet computationally-tractable for complex systems – trajectory-based strategies. In addition to the selected references in each Section, the reader seeking more general information can consult Refs. [38, 39, 40, 41, 42, 43]. Here, we restrict the discussion to some of the methods designed to solve the time-dependent Schrödinger equation for the molecular wavefunction. Methods aiming at describing the evolution of the density matrix or at the calculation of thermal correlation functions will not be described. The interested reader is referred to the abundant literature on this subject [44, 45, 46, 47, 48, 49, 50].

5.1.1 Quantum dynamics

Time-independent grid and basis set approaches. A *numerically-exact solution of the time-dependent Schrödinger equation* is possible, but only for a small number of nuclear degrees of freedom. The strategy consists first in discretizing the nuclear amplitudes, but also the different operators, on a numerical grid (Fig. 5), before performing the actual propagation of the nuclear wavefunctions. Such a discretization can be performed on a set of fixed *grid points* for each degree of freedom considered. While being rather straightforward, the use of a simple grid implies, among others, the use of finite differences to evaluate the effect of

differential operators.

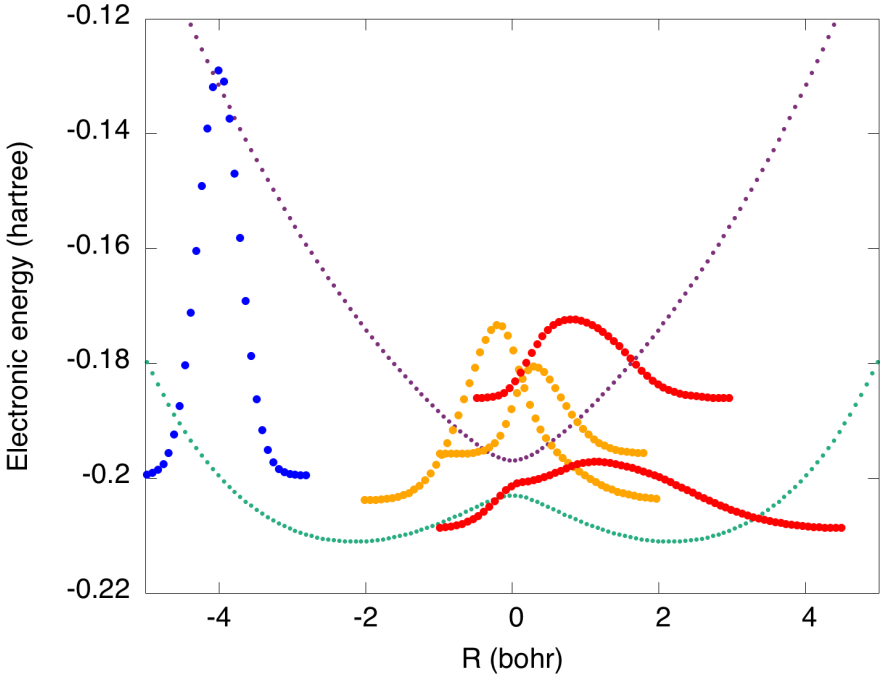

Figure 5: Schematic representation of a *grid-based quantum dynamics* version of the nonadiabatic dynamics presented in Fig. 3b. The PESs as well as the nuclear wavefunctions at three different times (t_0 = blue, t_1 = orange, and t_2 = red) are represented on a fixed grid (dots).

A more general approach to the quantum dynamics (QD) problem employs a *time-independent basis*, which means that the nuclear amplitudes are *discretized*, *i.e.*, each nuclear degree of freedom $(1, \ldots, f)$ is expressed in basis containing a certain number of functions $(N_1, \ldots, N_f$, respectively). The choice of the time-independent primitive basis functions depends on the problem investigated, and more information can be found in Refs. [51, 43]. Considering that each of the f degrees of freedom is expressed by N basis functions, the computational cost scales as N^f. Such an exponential scaling intrinsically restrains the application of numerically-exact quantum dynamics simulations to systems with a maximum of 10 degrees of freedom. As a result, a careful selection of the essential nuclear modes is required for studying the nonadiabatic dynamics of a molecule. Another critical step is the precalculation (plus fitting) of all the necessary electronic-structure information. The *diabatic* representation, in which the matrix of the kinetic energy operator is diagonal, is

preferred to the adiabatic one due to the smoothness of its PESs and couplings. Last but not least comes the final challenge of *integrating* the time-dependent Schrödinger equation, which takes a matrix-vector form when expressed in a basis [43]. Different integrators are available for this task like the split operator or Lanczos [52, 53].

As an example of the techniques described above, the quantum dynamics simulations presented in Figs. 2 were obtained by discretizing the molecular wavefunction on a grid (both for the electron and the moving proton), and integrating the Schrödinger equation using the split-operator integrator.

MultiConfiguration Time-Dependent Hartree. The MultiConfiguration Time-Dependent Hartree (MCTDH) [54, 55] introduces the use of *time-dependent* basis functions, called single-particle functions (SPFs), which are themselves written in a time-independent basis. Applying the Dirac-Frenkel variational principle within this definition gives a set of coupled equations of motion for both the complex amplitudes and the SPFs. The possibility for the SPFs to adapt in time usually results in a reduced number of basis functions, allowing to treat a larger number of nuclear degrees of freedom than with the time-independent basis approach. Additional strategies further allow to lower the computational cost of MCTDH [55], based for example on mode combination (dynamics with up to 30 modes) or multiple MCTDH layers (dynamics with > 100 modes) [56].

Trajectory basis functions. Another possible strategy to represent the nuclear wavefunctions consists in expressing them as linear combinations of so-called *trajectories basis functions* (TBFs), which are often taken as $3N_n$-dimensional Gaussians. The distinctive feature of the TBFs is that they can move in position and momentum space, following the nuclear wavefunctions and always offering a proper support for their propagation. In other words, one could picture the TBF as a moving grid. Using this representation for the nuclear amplitudes leads to a set of equations of motion for the complex expansion coefficients of the linear combination, that couples all the TBFs together – this is nothing but a Schrödinger equation in the basis of the TBFs. In the limit of a large number of TBFs, this representation would tend towards numerically-exact quantum dynamics. The idea, however, is that

we can reduce the number of TBFs to a small, tractable value *under the condition* that the TBFs closely follow the nuclear wavefunctions (thus reducing the number of Gaussians necessary to describe the dynamics as compared to a fixed grid). The challenge resides now in the definition of a set of equations of motion for the TBFs, which will fulfill this condition of a proper support for the nuclear wavefunctions, but at the lowest computational cost possible. The method called variational MultiConfiguration Gaussian (vMCG) [57] uses a Dirac-Frenkel variational principle, which ensures that the TBFs remain as close as possible to the nuclear wavefunctions during the dynamics [58]. In MultiConfiguration Ehrenfest (MCE) [59, 60], TBFs follow Ehrenfest trajectories (see below for more details on Ehrenfest dynamics) and have a frozen width, as proposed originally in the seminal work on TBFs by Heller [61, 62, 63]. Thanks to these two simplifications, the equations of motion for the TBFs are greatly simplified in MCE. Last but not least, Full Multiple Spawning (FMS) [64, 65] proposes to represent the nuclear amplitudes by a linear combination of frozen, classically-driven multidimensional Gaussians (Fig. 6). To overcome the challenge of having enough TBFs to support the nuclear dynamics, FMS introduces a spawning algorithm that allows for the addition of TBFs during the dynamics, *i.e.*, an adaptive size of the Gaussian basis, when the system reaches a region of strong nonadiabaticity [66, 67] (Fig. 6).

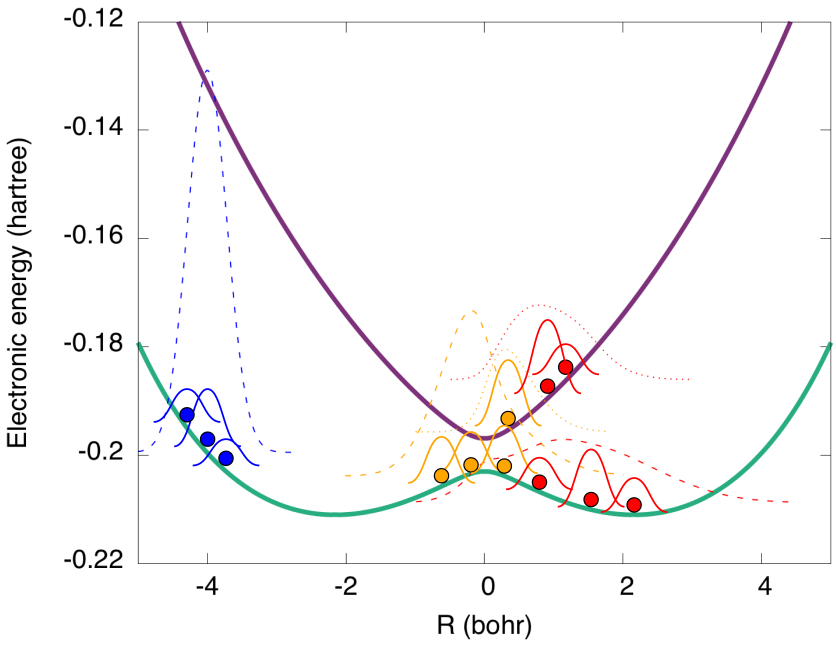

Figure 6: Schematic representation of the nonadiabatic dynamics presented in Fig. 3b using a method based on *trajectory basis functions* (here, Full Multiple Spawning). The nuclear wavefunctions (thin dashed lines) at three different times (t_0 = blue, t_1 = orange, and t_2 = red) are expressed on a basis of coupled TBFs (Gaussians with center indicated by a dot). New TBFs can be created in region of strong nonadiabatic couplings, and amplitude can be exchanged between the TBFs.

Importantly, vMCG, MCE, and FMS can formally reproduce a numerically exact solution of the time-dependent Schrödinger equation in the limit of a large number of TBFs (and an accurate calculation of their matrix elements). However, approximations can be devised to simplify the equations and allow for the nonadiabatic dynamics of molecules on-the-fly, leading to direct dynamics vMCG (DD-vMCG) [68, 58], Ab Initio MCE (AIMCE) [69], or Ab Initio Multiple Spawning (AIMS) [70, 71]. All three methods were successfully applied to problems in photochemistry and photophysics (see Ref. [67] for a list of the different molecular applications).

5.1.2 Mixed quantum/classical dynamics

The methods described before try to preserve the quantum nature of the nuclear degrees of freedom as much as possible. A pragmatic approach would consist in invoking a classical approximation for the nuclei while keeping a quantum, time-dependent, description of the electrons and an approximate description of nonadiabatic transitions. Such a *mixed quantum/classical* strategy propagates the nuclei as classical particles, *i.e.*, employing Newton's equation, but the potential energy from which the nuclear forces are derived can be different from the simple single adiabatic electronic state employed in Born-Oppenheimer molecular dynamics [72] to accommodate nonadiabatic effects [73, 74, 75].

A trajectory will be denoted $\mathbf{R}^\alpha(t)$, symbolizing the α realization of the nuclear configuration (position of all the nuclei of a molecule) at time t. The force $\mathbf{F}^\alpha(t)$ felt by the classical nuclei of the molecule at time t along the trajectory α is

$$\mathbf{F}^\alpha(t) = -\boldsymbol{\nabla}_\mathbf{R}\epsilon(\mathbf{R})|_{\mathbf{R}=\mathbf{R}^\alpha(t)}\,, \tag{10}$$

in which the form of the potential energy $\epsilon(\mathbf{R})$ still needs to be defined. The dynamics of the electrons will be dictated by the solution of a time-dependent electronic Schrödinger equation for the (time-dependent) electronic wavefunction $\Phi_{\mathbf{R}^\alpha(t)}(\mathbf{r},t)$, propagated on the support of the trajectory $\mathbf{R}^\alpha(t)$.

At this stage, the question is: *what should we choose for the electronic potential energy in Eq.* (10) *to drive the nuclear dynamics and incorporate nonadiabatic effects?* The following paragraphs introduce two possible answers to this question.

Ehrenfest dynamics. A first choice is to use the force

$$\mathbf{F}^\alpha(t) = \langle\Phi_{\mathbf{R}^\alpha(t)}(t)| - \boldsymbol{\nabla}_\mathbf{R}\hat{H}_{BO}(\mathbf{R}^\alpha(t))|\Phi_{\mathbf{R}^\alpha(t)}(t)\rangle_\mathbf{r}, \tag{11}$$

meaning that the classical trajectory follows a *mean-field potential energy*. Propagating a trajectory using Eq. (11) defines the mixed quantum/classical method called *Ehrenfest dynamics* [76, 77, 78, 79]. The electronic wavefunction $\Phi_{\mathbf{R}^\alpha(t)}(\mathbf{r},t)$ is propagated according to a time-dependent Schrödinger equation where an implicit dependence on time appears in the Hamiltonian *via* $\mathbf{R}^\alpha(t)$. From a more fundamental point of view, Ehrenfest dynamics

emerges from a classical limit applied on the nuclear degrees of freedom in the time-dependent self-consistent field method (TDSCF) [77, 72, 80].

The mean-field nature of Ehrenfest dynamics can lead to an artificial nuclear dynamics whenever the shapes of the PESs involved in the process under study strongly differ. However, when the different electronic states that can become coupled during the dynamics exhibit similar character, Ehrenfest dynamics can provide good results for short-time dynamics, in particular when the electronic dynamics can be solved efficiently, for example using TDDFT (see Refs. [81, 10] for examples).

Trajectory surface hopping. Another strategy to perform mixed quantum/classical dynamics would consist in propagating the trajectory on a given adiabatic PES, but offering it the possibility to *hop* between surfaces in case of strong nonadiabaticity. This idea is at the heart of the *Trajectory Surface Hopping* (TSH) method that was first proposed in the seventies [82, 83]. In TSH, the nuclear forces are computed from a stochastically-selected adiabatic PES after each nuclear integration time step:

$$\mathbf{F}^{\alpha}(t) = -\boldsymbol{\nabla}_{\mathbf{R}} \epsilon_{BO}^{(*)}(\mathbf{R})|_{\mathbf{R}=\mathbf{R}^{\alpha}(t)} \,. \tag{12}$$

In Eq. (12), $\epsilon_{BO}^{(*)}(\mathbf{R})$ indicates that the adiabatic PES used to propagate the trajectory α at time t needs to be defined. Hence, a *hopping criterion* is required, and the most commonly used approach is coined fewest-switches algorithm [84]. As in the case of Ehrenfest dynamics, a TSH run (there will be many, see below) consists in integrating a time-dependent electronic Schrödinger equation on the support of a classical trajectory. Conversely to Ehrenfest dynamics, though, in TSH the time-dependent electronic wavefunction is not directly used to produce forces on the classical nuclei, but mostly to detect regions of strong nonadiabaticity and to allow for hops between electronic states by changing the label $(*)$ of $\epsilon_{BO}^{(*)}(\mathbf{R})$ in Eq. (12). An important point of the TSH algorithm is that it requires a large number of *independent* trajectories, or independent TSH runs, to converge the hopping algorithm, as well as the sampling of initial conditions[7].

[7]The interested reader can consult for Refs. [41, 85, 36, 86, 87] for discussions on the importance of adequately selecting initial conditions for nonadiabatic dynamics.

Figure 7 shows schematically a swarm of independent TSH trajectories for our nonadiabatic model system. All the trajectories are initiated in S_0 at time t_0, evolving in the early time of the dynamics with nuclear forces (Eq. (12)) obtained from $\epsilon_{BO}^{(*)}(\mathbf{R}) = \epsilon_{BO}^{(S_0)}(\mathbf{R})$. At later time ($t_1$), some trajectories hop to S_1 and now feel the forces for this adiabatic state, while others carry their dynamics in S_0. The nuclear density can be reconstructed from the spatial distribution of classical trajectories, while counting the fraction of trajectories in each electronic state provides information about the electronic-state population.

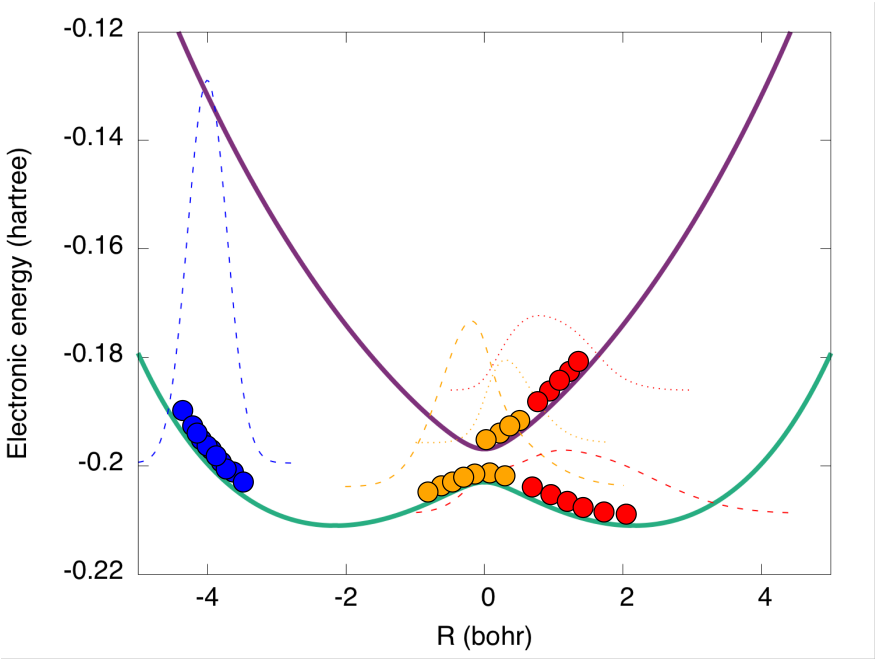

Figure 7: Schematic representation of the nonadiabatic dynamics presented in Fig. 3b using Trajectory Surface Hopping dynamics. A swarm of independent classical trajectories (circles) are initiated in S_0 at time t_0 (blue circles) and follow the adiabatic ground electronic state until the region of strong nonadiabaticity is reached (t_1, orange circles, and t_2, red circles) where hops between surfaces can be observed. The nuclear amplitudes (dashed and dotted lines) and adiabatic PECs (thick plain lines) are given for references.

The *independent trajectory approximation* inherent to TSH greatly simplifies the algorithm, but it also produces trajectories that are intrinsically overcoherent. In other words, TSH might suffer from a *decoherence* problem if a nuclear wavepacket branches after a nonadiabatic region, forming different wavepackets on different states that crosses the same

nonadiabatic regions again at later times. Due to the independent nature of the swarm of TSH trajectories, such decoherence is not accounted for in TSH [88, 89, 90, 91, 92, 93, 94, 95] at the level of the single trajectory[8]. Different corrections have been proposed to improve the overall result of TSH [96, 97, 98, 99, 100, 101, 102, 95, 103, 104], and we note that other approaches to surface hopping were discussed in the literature [105, 106].

Coupled-trajectory mixed quantum-classical algorithm. The coupled-trajectory mixed quantum-classical (CT-MQC) algorithm is the strategy that has been devised to solve the nuclear and electronic evolution equations (8) and (9) of the Exact Factorization employing an approximate trajectory-based description of the nuclei. The idea is to propagate trajectories based on the force computed from the time-dependent vector potential and the TDPES as schematically shown in Fig. 8. Tests on model systems have shown that those trajectories are able to follow, at least for short times, the evolution of the nuclear density [28, 27, 107, 108, 109, 110]. Furthermore, it has been proven that the trajectories evolved according to this *exact force* can be used to reconstruct the nuclear wavefunction $\chi(\mathbf{R},t)$, *i.e.*, the solution of the nuclear time-dependent Schrödinger equation (8) [18], and numerical tests have confirmed the validity of this property even for an approximate form of the force. The major difficulty resides in introducing suitable approximations to solve the electronic equation (9) in order to compute the conditional electronic wavefunction (a recent work proposed a detailed study of the mathematical and numerical stability properties of the Exact-Factorization equations [111]). For practical reasons, with the aim to exploit standard quantum-chemistry methods, a Born-Huang-like expansion is introduced for the conditional electronic wavefunction (rather than for the total wavefunction as discussed in Section 3).

The CT-MQC algorithm evolves classical-like trajectories in a way that looks similar to Ehrenfest dynamics (a time-dependent electronic wavefunction guides a classical trajectory), but with new terms that are typical of the Exact Factorization. In particular, the *quantum momentum* [22], derived from the term $-i\hbar[\nabla_\nu\chi(\mathbf{R},t)]/\chi(\mathbf{R},t)$ in the expression of the electron-nuclear coupling operator in Eq. (9), tracks the delocalization of the modulus of the

[8]Methods employing coupled trajectories, as those described in Section 5.1.1 for example, or methods based on TBFs would naturally include such decoherence effects.

nuclear wavefunction (or equivalently of the nuclear density). Therefore, the nuclear density has to be reconstructed at each time step of dynamics from the distribution of trajectories, to allow for the calculation of the quantum momentum [22, 112, 23, 113, 114]. This step in the algorithm requires that the trajectories are propagated simultaneously, somehow indirectly coupling them. If the quantum momentum is neglected, the trajectories are independent and the Ehrenfest algorithm is recovered [115, 116]. However, the coupling among the trajectories is essential to capture effects such as quantum decoherence [22, 23, 113].

While this brief description provides the general philosophy that led to the derivation of CT-MQC, a few additional approximations have been introduced to finalize the algorithm in a form that can be efficiently implemented in a molecular-dynamics code. Therefore, we refer to the literature on this topic for a detailed discussion [22, 112, 18, 10, 117, 118, 113].

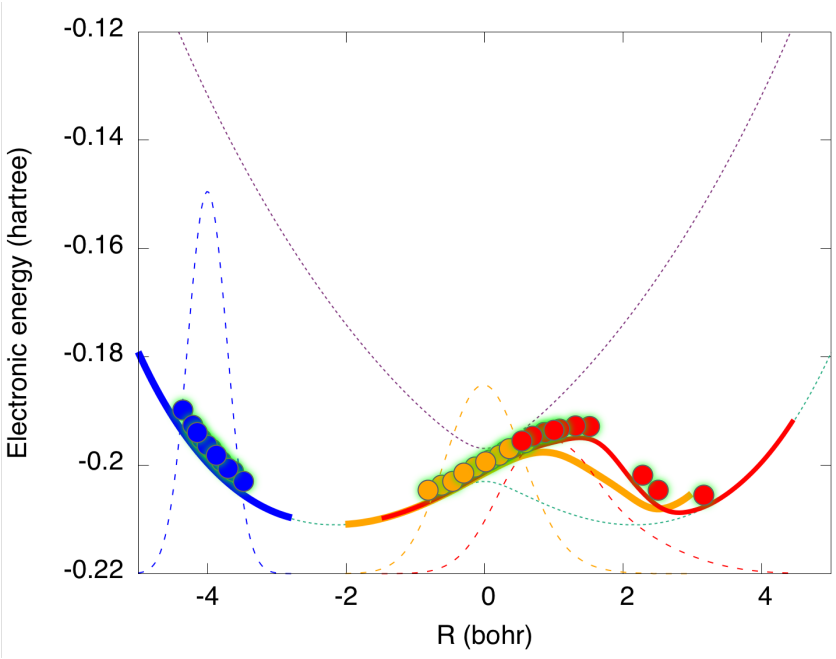

Figure 8: Schematic representation of the nonadiabatic dynamics presented in Fig. 4b in the framework of the Exact Factorization. Classical trajectories (filled circles, at times t_0 (blue), t_1 (orange) and t_2 (red)) propagated according to the CT-MQC algorithm follow the TDPES (colored plain lines), and are localized in the regions where the nuclear density (colored dashed lines) is large. The trajectories are coupled, and the coupling is indicated as the green area around each circle. The thin dotted lines are the adiabatic PECs shown as reference.

Other approaches to nonadiabatic molecular dynamics. Other alternative strategies were proposed to simulate nonadiabatic processes for molecules, and we reference some of them here for the interested reader. Semiclassical methods, which aim at approximating a quantum propagator in position space, have been extended to problems with multiple electronic states [119, 120, 121, 122, 123, 124, 125, 126]. Quantum (or Bohmian) trajectories were also proposed as a mean to go beyond the independent trajectory approximation of TSH [127, 128, 129, 91, 130]. Algorithms have also been proposed exploiting the idea of conditional electronic wavefunctions [130, 131, 132].

6 Applications of nonadiabatic molecular dynamics

The different methods for nonadiabatic dynamics introduced above have been successfully employed to simulate the excited-state dynamics of molecular systems. This section aims at offering some selected examples of the types of photophysical and photochemical processes described by these techniques. For a more extended list of applications, the reader can refer to Refs. [133, 41] (for quantum dynamics), Ref. [133, 58, 60, 67] (for travelling Gaussian techniques), or Refs. [134, 133, 135, 41, 36] (for mixed quantum/classical methods).

Most methods described above have been employed to study different types of processes like photoexcitation, internal conversion, and intersystem crossing processes. The complex photodissociation dynamics of the organometallic compound $CpMnCO_5$ triggered by an optimal laser pulse was rationalized by means of quantum dynamics simulations in a reduced number of dimensions [136]. Quantum dynamics simulations also provide access to vibronically resolved photoabsorption and photoelectron spectra. In a recent work, the photoelectron spectrum of phenol was accurately reproduced using MCTDH combined with a vibronic-coupling Hamiltonian composed of 7 vibrational modes and constructed based on CASSCF data, further allowing for the identification of a conical intersection between the ionized states [137]. AIMS is a powerful method to investigate the nonadiabatic dynamics of medium-size molecules in their full configuration space. For example, AIMS has been successfully used to compute and interpret experimental observables [138, 139], and even predict them [140] years before their actual experimental measurement [141]. The mechanism of photoinduced energy transfer between the building blocks in a phenylene ethynylene dendrimer was identified by using a special variant of AIMCE, employing a time-dependent diabatic basis [142]. The complex excited-state dynamics of formamide, comprising eight coupled electronic states, was investigated using DD-vMCG dynamics. This method was also employed to study the electron wavepacket dynamics of paraxylene and modified bis-methylene-adamantane following their ionization [143]. Among its numerous applications, TSH was for example used to understand the dynamics of the retinal chromophore through a conical intersection, using a QM/MM formalism, or to investigate the role the intersystem crossing of $Ru[bpy]_3^{2+}$ in gas phase [144] and water [145]. Ehrenfest dynamics is particularly

well suited to study the early dynamics of an approximate electronic wavepacket dynamics generated by collisions with heavily charged ions [146], or following a photoionization triggered by attosecond (broadband) pulses [147]. CT-MQC is well-suited to describe processes where decoherence effects are significant and has been recently applied to study the photoinduced ring-opening process in oxirane [23, 24].

6.1 Box: Experimental observation of ultrafast dynamics through conical intersections

The recent development of novel experimental techniques like ultrafast X-ray diffraction or ultrafast electron diffraction (UED) has opened new doors to observe experimentally the ultrafast processes following photoexcitation of molecules. In particular, they offer time-resolved structural information that can directly be compared with the result of nonadiabatic quantum dynamics, as exemplified by the excited-state dynamics of I_2 [148] (QD and UED), the photodissociation and dynamics through a conical intersection of CF_3I (UED and AIMS) [149], or the photoinduced ring-opening of cyclohexadiene [150] (UED and AIMS).

7 Summary and Outlook

In this Overview, we have discussed the theoretical description of nonadiabatic dynamics from the perspective of the time-dependent molecular wavefunction. The Born-Huang representation of the molecular wavefunction gives rise to our current vision of photochemical and photophysical processes, with nuclear wavefunctions evolving on (time-independent) electronic states and exchanging amplitudes due to nonadiabatic couplings. The Exact Factorization of the molecular wavefunction introduces a different vision, where a nuclear wavefunction evolves under the influence of a single time-dependent potential energy surface and vector potential. Based on these representations, various strategies were introduced to perform, or approximate, the nuclear dynamics of molecules in nonadiabatic conditions.

Nonadiabatic dynamics is a very active field of research, and we outline here some recent new directions. A recently developed method, SQC/MM [151], combines a Meyer-Miller

classical representation of both the electronic and the nuclear degrees of freedom [152] with a symmetrical quasi-classical Meyer-Miller (SQC) windowing model [153, 154] to describe nonadiabatic dynamics. New developments merging the ideas of vMCG, Ehrenfest dynamics, and the Exact Factorization are ongoing [155]. The idea of moving beyond the use of a purely adiabatic electronic basis with traveling Gaussian functions has triggered interesting new work in the last years [156, 157, 158, 159]. Considerable efforts have been invested more recently in developing a robust algorithm for performing MCTDH on-the-fly [160]. Nonadiabatic molecular dynamics combined with machine-learning strategies for the calculation of electronic-structure quantities has recently emerged [161, 162, 163]. Quantum electrodynamics effects have been introduced in nonadiabatic dynamics, like for example molecular dynamics in an optical cavity [164, 165] or the description of stimulated emission processes [166].

The recent advancements in ultrafast spectroscopy combined with the importance of light-triggered phenomena in chemical applications will surely further amplify the interest for the development of techniques for nonadiabatic molecular dynamics.

8 Acknowledgements

BFEC acknowledges support from Durham University.

9 Conflict of interest

The authors have declared no conflicts of interest for this article.

References

[1] J C Tully. Perspective on "Zur Quantentheorie der Molekeln". Theor. Chem. Acc., 103(3):173–176, 2000.

[2] L K McKemmish, R H McKenzie, N S Hush, and J R Reimers. Electron–vibration

entanglement in the born–oppenheimer description of chemical reactions and spectroscopy. Phys. Chem. Chem. Phys., 17(38):24666–24682, 2015.

[3] J R Reimers, L K McKemmish, R H McKenzie, and N S Hush. Non-adiabatic effects in thermochemistry, spectroscopy and kinetics: the general importance of all three born–oppenheimer breakdown corrections. Phys. Chem. Chem. Phys., 17(38):24641–24665, 2015.

[4] C Xie, C L Malbon, D R Yarkony, D Xie, and H Guo. Signatures of a conical intersection in adiabatic dissociation on the ground electronic state. J. Am. Chem. Soc., 140 (6):1986–1989, 2018.

[5] S Shin and H Metiu. Nonadiabatic effects on the charge transfer rate constant: A numerical study of a simple model system. J. Chem. Phys., 102(23):9285–9295, 1995.

[6] M. Born and R. Oppenheimer. Zur Quantentheorie der Molekeln. Ann. Phys., 389 (20):457–484, 1927.

[7] F. G. Eich and F. Agostini. The adiabatic limit of the exact factorization of the electron-nuclear wave function. J. Chem. Phys., 145:054110, 2016.

[8] M. Born and K. Huang. Dynamical Theory of Crystal Lattices. Clarendon, Oxford, 1954.

[9] G. A. Worth and L. S. Cederbaum. Beyond Born-Oppenheimer: molecular dynamics through a conical intersection. Annu. Rev. Phys. Chem., 55:127–158, 2004.

[10] F. Agostini, B. F. E. Curchod, R. Vuilleumier, I. Tavernelli, and E. K. U. Gross. TDDFT and quantum-classical dynamics: A universal tool describing the dynamics of matter. In Wanda Andreoni and Sidney Yip, editors, Handbook of Materials Modeling, pages 1–47. Springer Netherlands, 2018.

[11] A. Abedi, N. T. Maitra, and E. K. U. Gross. Exact factorization of the time-dependent electron-nuclear wave function. Phys. Rev. Lett., 105(12):123002, 2010.

[12] A. Abedi, N. T. Maitra, and E. K. U. Gross. Correlated electron-nuclear dynamics: Exact factorization of the molecular wave-function. J. Chem. Phys., 137(22):22A530, 2012.

[13] G. Hunter. Conditional probability amplitude analysis of coupled harmonic oscillators. Int. J. Quantum Chem., 8:413–420, 1974.

[14] G. Hunter. Conditional probability amplitudes in wave mechanics. Int. J. Quantum Chem., 9:237–242, 1975.

[15] G. Hunter. Nodeless wave function quantum theory. Int. J. Quantum Chem., 9:133, 1980.

[16] G. Hunter. Nodeless wave functions and spiky potentials. Int. J. Quantum Chem., 19: 755–761, 1981.

[17] G. Hunter and C. C. Tai. Variational marginal amplitudes. Int. J. Quantum Chem., 21:1041–1050, 1982.

[18] F. Agostini, I. Tavernelli, and G. Ciccotti. Nuclear quantum effects in electronic (non)adiabatic dynamics. Euro. Phys. J. B, 91:139, 2018.

[19] B. F. E. Curchod and F. Agostini. On the dynamics through a conical intersection. J. Phys. Chem. Lett., 8:831–837, 2017.

[20] F. Agostini and B. F. E. Curchod. When the exact factorization meets conical intersections... Euro. Phys. J. B, 91:141, 2018.

[21] S. K. Min, A. Abedi, K. S. Kim, and E. K. U. Gross. Is the molecular berry phase an artefact of the born-oppenheimer approximation? Phys. Rev. Lett., 113(26):263004, 2014.

[22] S. K. Min, F. Agostini, and E. K. U. Gross. Coupled-trajectory quantum-classical approach to electronic decoherence in nonadiabatic processes. Phys. Rev. Lett., 115 (7):073001, 2015.

[23] S. K. Min, F. Agostini, I. Tavernelli, and E. K. U. Gross. Ab initio nonadiabatic dynamics with coupled trajectories: A rigorous approach to quantum (de)coherence. J. Phys. Chem. Lett., 8:3048–3055, 2017.

[24] B. F. E. Curchod, F. Agostini, and I. Tavernelli. CT-MQC – A coupled-trajectory mixed quantum/classical method including nonadiabatic quantum coherence effects. Euro. Phys. J. B, 91:168, 2018.

[25] R. Requist and E. K. U. Gross. Exact factorization-based density functional theory of electrons and nuclei. Phys. Rev. Lett., 117:193001, 2016.

[26] C. Li, R. Requist, and E. K. U. Gross. Density functional theory of electron transfer beyond the Born-Oppenheimer approximation: Case study of LiF. J. Chem. Phys., 148:084110, 2018.

[27] F. Agostini, A. Abedi, Y. Suzuki, S. K. Min, N. T. Maitra, and E. K. U. Gross. The exact forces on classical nuclei in non-adiabatic charge transfer. J. Chem. Phys., 142 (8):084303, 2015.

[28] F. Agostini, A. Abedi, Y. Suzuki, and E. K. U. Gross. Mixed quantum-classical dynamics on the exact time-dependent potential energy surfaces: A novel perspective on non-adiabatic processes. Mol. Phys., 111(22-23):3625–3640, 2013.

[29] W. Domcke, D. Yarkony, and H. Köppel, editors. Conical Intersections: Electronic Structure, Dynamics & Spectroscopy, volume 15. World Scientific Pub Co Inc, 2004.

[30] M Merchán and L Serrano-Andrés. II. ab initio methods for excited states. In M. Olivucci, editor, Computational Photochemistry, volume 16 of Theoretical and Computational Chemistry, pages 35 – 91. Elsevier, 2005.

[31] L. González, D. Escudero, and L. Serrano-Andrés. Progress and challenges in the calculation of electronic excited states. ChemPhysChem, 13(1):28–51, 2012.

[32] H Lischka, D Nachtigallová, A J A Aquino, P G Szalay, F Plasser, F B C Machado, and M Barbatti. Multireference approaches for excited states of molecules. Chem. Rev., 118:7293, 2018.

[33] C A Ullrich. Time-Dependent Density-Functional Theory. Oxford University Press, 2012.

[34] M. Barbatti, R. Shepard, and H. Lischka. Computational and methodological elements for nonadiabatic trajectory dynamics simulations of molecules. In W. Domcke, D. R. Yarkony, and H. Koeppel, editors, Conical Intersections: Theory, Computation and Experiment, page 415. Singapore, World Scientific, 2011.

[35] P G Szalay, T Müller, G Gidofalvi, H Lischka, and R Shepard. Multiconfiguration self-consistent field and multireference configuration interaction methods and applications. Chem. Rev., 112(1):108–181, 2011.

[36] R Crespo-Otero and M Barbatti. Recent advances and perspectives on nonadiabatic mixed quantum–classical dynamics. Chem. Rev., 118:7026–7068, 2018.

[37] A Dreuw and M Wormit. The algebraic diagrammatic construction scheme for the polarization propagator for the calculation of excited states. WIREs Comput. Mol. Sci., 5(1):82–95, 2015.

[38] J C Tully. Perspective: Nonadiabatic dynamics theory. J. Chem. Phys., 137(22): 22A301, 2012.

[39] F Hagelberg. Electron dynamics in molecular interactions: principles and applications. World Scientific, 2013.

[40] J P Malhado, M J Bearpark, and J T Hynes. Non-adiabatic dynamics close to conical intersections and the surface hopping perspective. Front. Chem., 2:97, 2014.

[41] M Persico and G Granucci. An overview of nonadiabatic dynamics simulations methods, with focus on the direct approach versus the fitting of potential energy surfaces. Theor. Chem. Acc., 133(9):1–28, 2014.

[42] F Gatti. Molecular quantum dynamics: from theory to applications. Springer, 2014.

[43] F Gatti, B Lasorne, H-D Meyer, and A Nauts. Applications of Quantum Dynamics in Chemistry, volume 98. Springer, 2017.

[44] P Huo and D F Coker. Consistent schemes for non-adiabatic dynamics derived from partial linearized density matrix propagation. J. Chem. Phys., 137:22A535, 2012.

[45] E. R. Dunkel, S. Bonella, and D. F. Coker. Iterative linearized approach to nonadiabatic dynamics. J. Chem. Phys., 129:114106, 2008.

[46] R Kapral and G Ciccotti. Mixed quantum-classical dynamics. J. Chem. Phys., 110: 8919, 1999.

[47] S Jang. Nonadiabatic quantum Liouville and master equations in the adiabatic basis. J. Chem. Phys., 137:22A536, 2012.

[48] Raymond Kapral. Progress in the theory of mixed quantum-classical dynamics. Annu. Rev. Phys. Chem., 57:129–157, 2006.

[49] S Bonella, G Ciccotti, and R Kapral. Linearization approximations and liouville quantum–classical dynamics. Chem. Phys. Lett., 484(4-6):399–404, 2010.

[50] W C Pfalzgraff, A Kelly, and T E Markland. Nonadiabatic dynamics in atomistic environments: harnessing quantum-classical theory with generalized quantum master equations. J. Phys. Chem. Lett., 6(23):4743–4748, 2015.

[51] D J. Tannor. Introduction to quantum mechanics, a time-dependent perspective. University Science Books, Sausalito, California, 2007.

[52] R Kosloff. Time-dependent quantum-mechanical methods for molecular dynamics. J. Phys. Chem., 92(8):2087–2100, 1988.

[53] R Kosloff. Propagation methods for quantum molecular dynamics. Annu. Rev. Phys. Chem., 45(1):145–178, 1994.

[54] M. H. Beck, A. Jäckle, G. A. Worth, and H. D. Meyer. The multiconfiguration time-dependent hartree (MCTDH) method: a highly efficient algorithm for propagating wavepackets. Phys. Rep., 324(1):1–105, 2000.

[55] H-D Meyer, F Gatti, and G A Worth. Multidimensional quantum dynamics. John Wiley & Sons, 2009.

[56] H Wang and M Thoss. Multilayer formulation of the multiconfiguration time-dependent hartree theory. J. Chem. Phys., 119(3):1289–1299, 2003.

[57] GA Worth, MA Robb, and I Burghardt. A novel algorithm for non-adiabatic direct dynamics using variational Gaussian wavepackets. Faraday Discuss., 127:307–323, 2004.

[58] GW Richings, I Polyak, KE Spinlove, GA Worth, I Burghardt, and B Lasorne. Quantum dynamics simulations using gaussian wavepackets: the vmcg method. Int. Rev. Phys. Chem., 34(2):269–308, 2015.

[59] D.V. Shalashilin. Quantum mechanics with the basis set guided by ehrenfest trajectories: Theory and application to spin-boson model. J. Chem. Phys., 130:244101, 2009.

[60] D Makhov, C Symonds, S Fernandez-Alberti, and D Shalashilin. Ab initio quantum direct dynamics simulations of ultrafast photochemistry with multiconfigurational ehrenfest approach. Chem. Phys., 493:200, 2017.

[61] E. J. Heller. Time-dependent approach to semiclassical dynamics. J. Chem. Phys., 62: 1544–1555, 1975.

[62] E J Heller. The semiclassical way to molecular spectroscopy. Acc. Chem. Res., 14(12): 368–375, 1981.

[63] E J Heller. Frozen gaussians: A very simple semiclassical approximation. J. Chem. Phys., 75(6):2923–2931, 1981.

[64] T. J. Martínez, M. Ben-Nun, and R D Levine. Multi-electronic-state molecular dynamics: A wave function approach with applications. J. Phys. Chem., 100(19):7884–7895, 1996.

[65] T. J. Martínez and R D Levine. Non-adiabatic molecular dynamics: Split-operator multiple spawning with applications to photodissociation. J. Chem. Soc., Faraday Trans., 93(5):941–947, 1997.

[66] M Ben-Nun and T. J. Martínez. Ab initio quantum molecular dynamics. Adv. Chem. Phys., 121:439–512, 2002.

[67] B F E Curchod and T J Martínez. Ab initio nonadiabatic quantum molecular dynamics. Chem. Rev., 118(7):3305–3336, 2018.

[68] B Lasorne, M J Bearpark, M A Robb, and G A Worth. Direct quantum dynamics using variational multi-configuration gaussian wavepackets. Chem. Phys. Lett., 432 (4):604–609, 2006.

[69] K Saita and D V Shalashilin. On-the-fly ab initio molecular dynamics with multiconfigurational ehrenfest method. J. Chem. Phys., 137(22):22A506, 2012.

[70] M. Ben-Nun and Todd J. Martínez. Nonadiabatic molecular dynamics: Validation of the multiple spawning method for a multidimensional problem. J. Chem. Phys., 108: 7244–7257, 1998.

[71] M. Ben-Nun, J. Quenneville, and T. J. Martínez. Ab initio multiple spawning: Photochemistry from first principles quantum molecular dynamics. J. Phys. Chem. A, 104: 5161–5175, 2000.

[72] D. Marx and J. Hutter. Ab Initio Molecular Dynamics: Basic Theory and Advanced Methods. Cambridge University Press, 2009.

[73] J. C. Tully. Nonadiabatic dynamics. In D. L. Thompson, editor, Modern Methods for Multidimensional Dynamics Computations in Chemistry. Singapore, World Scientific, 1998.

[74] J C. Tully. Mixed quantum classical dynamics. Faraday Discuss., 110:407, 1998.

[75] M. D. Hack and D. G. Truhlar. Nonadiabatic trajectories at an exhibition. J. Phys. Chem. A, 104:7917–7926, 2000.

[76] J B Delos, W R Thorson, and S K Knudson. Semiclassical theory of inelastic collisions. i. classical picture and semiclassical formulation. Physical Review A, 6(2):709, 1972.

[77] J. C. Tully. In B. J. Berne, G. Ciccotti, and D. F. Coker, editors, Classical and Quantum Dynamics in Condensed Phase Simulations. Singapore, World Scientific, 1998.

[78] X Li, J C. Tully, H. B Schlegel, and M J. Frisch. Ab initio Ehrenfest dynamics. J. Chem. Phys., 123(8):084106, 2005.

[79] T Yonehara, K Hanasaki, and K Takatsuka. Fundamental approaches to nonadiabaticity: Toward a chemical theory beyond the Born-Oppenheimer paradigm. Chem. Rev., 112(1):499–542, 2012.

[80] F Agostini, E.K.U. Gross, and B F. E. Curchod. Electron-nuclear entanglement in the time-dependent molecular wavefunction. Comput. Theor. Chem., page 10.1016/j.comptc.2019.01.021, 2019.

[81] X. Andrade, A. Castro, D. Zueco, J.L. Alonso, P. Echenique, F. Falceto, and A. Rubio. Modified Ehrenfest formalism for efficient large-scale ab initio molecular dynamics. J. Chem. Theory Comput., 5(4):728–742, 2009.

[82] A Bjerre and EE Nikitin. Energy transfer in collisions of an excited sodium atom with a nitrogen molecule. Chem. Phys. Lett., 1(5):179–181, 1967.

[83] J C. Tully and R K. Preston. Trajectory surface hopping approach to nonadiabatic molecular collisions: The reaction of H^+ with D_2. J. Chem. Phys., 55(2):562–572, 1971.

[84] J. C. Tully. Molecular dynamics with electronic transitions. J. Chem. Phys., 93: 1061–1071, 1990.

[85] M Barbatti and K Sen. Effects of different initial condition samplings on photodynamics and spectrum of pyrrole. Int. J. Quantum Chem., 116(10):762–771, 2016.

[86] J Suchan, D Hollas, B F. E. Curchod, and P Slavicek. On the importance of initial conditions for excited-state dynamics. Faraday Discuss., 2018.

[87] S Mai, H Gattuso, A Monari, and L González. Novel molecular-dynamics-based protocols for phase space sampling in complex systems. Front. Chem., 6:495, 2018.

[88] A W Jasper, S Nangia, C Zhu, and D G Truhlar. Non-Born-Oppenheimer molecular dynamics. Acc. Chem. Res., 39:101, 2006.

[89] G Granucci and M Persico. Critical appraisal of the fewest switches algorithm for surface hopping. J. Chem. Phys., 126:134114, 2007.

[90] H M Jaeger, S Fischer, and O V Prezhdo. Decoherence-induced surface hopping. J. Chem. Phys., 137:22A545, 2012.

[91] B F E Curchod and I Tavernelli. On trajectory-based nonadiabatic dynamics: Bohmian dynamics versus trajectory surface hopping. J. Chem. Phys., 138:184112, 2013.

[92] J E Subotnik, W Ouyang, and B R Landry. Can we derive Tully's surface-hopping algorithm from the semiclassical quantum Liouville equation? Almost, but only with decoherence. J. Chem. Phys., 139:214107, 2013.

[93] X Gao and W Thiel. Non-hermitian surface hopping. Phys. Rev. E, 95:013308, 2017.

[94] B J Schwartz, E R Bittner, O V Prezhdo, and P J Rossky. Quantum decoherence and the isotope effect in condensed phase nonadiabatic molecular dynamics simulations. J. Chem. Phys., 104:5942, 1996.

[95] J-Y Fang and S Hammes-Schiffer. Improvement of the internal consistency in trajectory surface hopping. J. Phys. Chem. A, 103:9399–9407, 1999.

[96] A W Jasper and D G Truhlar. Electronic decoherence time for non-born-oppenheimer trajectories. J. Chem. Phys., 127:194306, 2007.

[97] G. Granucci, M. Persico, and A. Zoccante. Including quantum decoherence in surface hopping. J. Chem. Phys., 133:134111, 2010.

[98] N. Shenvi, J. E. Subotnik, and W. Yang. Simultaneous-trajectory surface hopping: A parameter-free algorithm for implementing decoherence in nonadiabatic dynamics. J. Chem. Phys., 134:144102, 2011.

[99] N. Shenvi, J. E. Subotnik, and W. Yang. Phase-corrected surface hopping: Correcting the phase evolution of the electronic wavefunction. J. Chem. Phys., 135:024101, 2011.

[100] N. Shenvi and W. Yang. Achieving partial decoherence in surface hopping through phase correction. J. Chem. Phys., 137:22A528, 2012.

[101] J. E. Subotnik and N. Shenvi. A new approach to decoherence and momentum rescaling in the surface hopping algorithm. J. Chem. Phys., 134:024105, 2011.

[102] J E Subotnik and N Shenvi. Decoherence and surface hopping: When can averaging over initial conditions help capture the effects of wave packet separation? J. Chem. Phys., 134:244114, 2011.

[103] I Horenko, C Salzmann, B Schmidt, and C Schutte. Quantum-classical Liouville approach to molecular dynamics: Surface hopping Gaussian phase-space packets. J. Chem. Phys., 117(24):11075–11088, 2002.

[104] A W Jasper, S N Stechmann, and D G Truhlar. Fewest-switches with time uncertainty: A modified trajectory surface-hopping algorithm with better accuracy for classically forbidden electronic transitions. J. Chem. Phys., 116(13):5424–5431, 2002.

[105] S Nielsen, R Kapral, and G Ciccotti. Mixed quantum-classical surface hopping dynamics. J. Chem. Phys., 112:6543–6553, 2000.

[106] C C Martens. Surface hopping by consensus. J. Phys. Chem. Lett., 7(13):2610–2615, 2016.

[107] F. Agostini, S. K. Min, and E. K. U. Gross. Semiclassical analysis of the electron-nuclear coupling in electronic non-adiabatic processes. Ann. Phys., 527(9-10):546–555, 2015.

[108] Y. Suzuki, A. Abedi, N. T. Maitra, and E. K. U. Gross. Laser-induced electron localization in H_2^+: Mixed quantum-classical dynamics based on the exact time-dependent potential energy surface. Phys. Chem. Chem. Phys., 17:29271–29280, 2015.

[109] Y. Suzuki and K. Watanabe. Bohmian mechanics in the exact factorization of electron-nuclear wave functions. Phys. Rev. A, 94:032517, 2016.

[110] B. F. E. Curchod, F. Agostini, and E. K. U. Gross. An exact factorization perspective on quantum interferences in nonadiabatic dynamics. J. Chem. Phys., 145:034103, 2016.

[111] Graeme H Gossel, Lionel Lacombe, and Neepa T Maitra. On the numerical solution of the exact factorization equations. arXiv preprint arXiv:1901.11216, 2019.

[112] F. Agostini, S. K. Min, A. Abedi, and E. K. U. Gross. Quantum-classical non-adiabatic dynamics: Coupled- vs. independent-trajectory methods. J. Chem. Theory Comput., 12(5):2127–2143, 2016.

[113] J.-K. Ha, I. S. Lee, and S. K. Min. Surface hopping dynamics beyond nonadiabatic couplings for quantum coherence. J. Phys. Chem. Lett., 9:1097–1104, 2018.

[114] B. Gu and I. Franco. Partial hydrodynamic representation of quantum molecular dynamics. J. Chem. Phys., 146:194104, 2017.

[115] F. Agostini, A. Abedi, and E. K. U. Gross. Classical nuclear motion coupled to electronic non-adiabatic transitions. J. Chem. Phys., 141(21):214101, 2014.

[116] A. Abedi, F. Agostini, and E. K. U. Gross. Mixed quantum-classical dynamics from the exact decomposition of electron-nuclear motion. Europhys. Lett., 106(3):33001, 2014.

[117] F. Agostini. An exact-factorization perspective on quantum-classical approaches to excited-state dynamics. Euro. Phys. J. B, 91:143, 2018.

[118] G. Gossel, F. Agostini, and N. T. Maitra. Coupled-trajectory mixed quantum-classical algorithm: A deconstruction. J. Chem. Theory Comput., 14:4513–4529, 2018.

[119] J. Schwinger. Quantum Theory of Angular Momentum. Academic New York, l. c. biedenharn and h. v. dam edition, 1965.

[120] C. W. McCurdy, H. D. Meyer, and W. H. Miller. Classical model for electronic degrees of freedom in nonadiabatic collision processes: Pseudopotential analysis and calculations for F($^2P_{1/2} + H^+$), Xe→F($^2P_{3/2} + H^+$),Xe. J. Chem. Phys., 70:3177–3187, 1979.

[121] G. Stock and M. Thoss. Semiclassical description of nonadiabatic quantum dynamics. Phys. Rev. Lett., 78:578, 1997.

[122] X. Sun and W. H. Miller. Semiclassical initial value representation for electronically nonadiabatic molecular dynamics. J. Chem. Phys., 106:6346, 1997.

[123] M. Thoss and G. Stock. Mapping approach to the semiclassical description of nonadiabatic quantum dynamics. Phys. Rev. A, 59:64, 1999.

[124] M. Thoss, W. H. Miller, and G. Stock. Semiclassical description of nonadiabatic quantum dynamics: Application to the S1-S2 conical intersection in pyrazine. J. Chem. Phys., 112:10282, 2000.

[125] W. H. Miller. Electronically nonadiabatic dynamics via semiclassical initial value methods. J. Phys. Chem. A, 113:1405–1415, 2009.

[126] M. Thoss and H. Wang. Semiclassical description of molecular dynamics based on initial-value representation methods. Annu. Rev. Phys. Chem., 55:299–332, 2004.

[127] R E. Wyatt, C L. Lopreore, and G Parlant. Electronic transitions with quantum trajectories. J. Chem. Phys., 114(12):5113–5116, 2001.

[128] B Poirier and G Parlant. Reconciling semiclassical and Bohmian mechanics: IV. Multisurface dynamics. J. Phys. Chem. A, 111(41):10400–10408, 2007.

[129] V A. Rassolov and S Garashchuk. Semiclassical nonadiabatic dynamics with quantum trajectories. Phys. Rev. A, 71(3):032511, 2005.

[130] G Albareda, H Appel, I Franco, A Abedi, and A Rubio. Correlated electron-nuclear dynamics with conditional wave functions. Phys. Rev. Lett., 113(8):083003, 2014.

[131] G Albareda, J M Bofill, I Tavernelli, F Huarte-Larrañaga, F Illas, and A Rubio. Conditional born-oppenheimer dynamics: Quantum dynamics simulations for the model Porphine. J. Phys. Chem. Lett., 6:1529, 2015.

[132] G Albareda, A Kelly, and A Rubio. Nonadiabatic quantum dynamics without potential energy surfaces. Phys. Rev. Materials, 3:023803, 2019.

[133] B Lasorne, G A. Worth, and M A. Robb. Excited-state dynamics. WIREs Comput. Mol. Sci., 1(3):460–475, 2011. ISSN 1759-0884.

[134] M Barbatti. Nonadiabatic dynamics with trajectory surface hopping method. WIREs Comput. Mol. Sci., 1:620–633, 2011. ISSN 1759-0884.

[135] B F E Curchod, U Rothlisberger, and I Tavernelli. Trajectory-based nonadiabatic dynamics with time-dependent density functional theory. ChemPhysChem, 14(7):1314–1340, 2013.

[136] C. Daniel, L. González, C. Lupulescu, J. Manz, A. Merli, Š. Vajda, L. Wöste, et al. Deciphering the reaction dynamics underlying optimal control laser fields. Science, 299 (5606):536, 2003.

[137] MP Taylor and GA Worth. Vibronic coupling model to calculate the photoelectron spectrum of phenol. Chem. Phys., 2018.

[138] H Tao, TK Allison, TW Wright, AM Stooke, C Khurmi, J Van Tilborg, Y Liu, RW Falcone, A Belkacem, and TJ Martinez. Ultrafast internal conversion in ethylene. i. the excited state lifetime. J. Chem. Phys., 134(24):244306, 2011.

[139] W J Glover, T Mori, M S Schuurman, A E Boguslavskiy, O Schalk, A Stolow, and T J Martínez. Excited state non-adiabatic dynamics of the smallest polyene, trans 1, 3-butadiene. ii. ab initio multiple spawning simulations. J. Chem. Phys., 148(16): 164303, 2018.

[140] T Mori, W J Glover, M S Schuurman, and T J Martinez. Role of rydberg states in the photochemical dynamics of ethylene. The Journal of Physical Chemistry A, 116(11): 2808–2818, 2012.

[141] T Kobayashi, T Horio, and T Suzuki. Ultrafast deactivation of the $\pi\pi^*$(v) state of ethylene studied using sub-20 fs time-resolved photoelectron imaging. J. Phys. Chem. A, 119(36):9518–9523, 2015.

[142] S Fernandez-Alberti, D V Makhov, S Tretiak, and D V Shalashilin. Non-adiabatic excited state molecular dynamics of phenylene ethynylene dendrimer using a multi-configurational ehrenfest approach. Phys. Chem. Chem. Phys., 18(15):10028–10040, 2016.

[143] M Vacher, M J Bearpark, M A Robb, and J P Malhado. Electron dynamics upon ionization of polyatomic molecules: Coupling to quantum nuclear motion and decoherence. Phys. Rev. Lett., 118(8):083001, 2017.

[144] A J Atkins and L González. Trajectory surface-hopping dynamics including intersystem crossing in [Ru(bpy)3]2+. J. Phys. Chem. Lett., 8(16):3840–3845, 2017.

[145] I. Tavernelli, B. F. E. Curchod, and U. Rothlisberger. Nonadiabatic molecular dynamics with solvent effects: a LR-TDDFT QM/MM study of ruthenium (II) tris (bipyridine) in water. Chem. Phys., 391:101, 2011.

[146] P. Lopez-Tarifa, M.-A. Herve du Penhoat, R. Vuilleumier, M.-P. Gaigeot, I. Tavernelli, A. Le Padellec, J.-P. Champeaux, M. Alcami, P. Moretto-Capelle, F. Martin, and M.-F. Politis. Ultrafast nonadiabatic fragmentation dynamics of doubly charged uracil in a gas phase. Phys. Rev. Lett., 107:023202, 2011.

[147] M Lara-Astiaso, M Galli, A Trabattoni, A Palacios, D Ayuso, F Frassetto, L Poletto, S De Camillis, J Greenwood, P Decleva, I Tavernelli, F Calegari, M Nisoli, and F Martin. Attosecond pump–probe spectroscopy of charge dynamics in tryptophan. J. Phys. Chem. Lett., 9(16):4570–4577, 2018.

[148] J Yang, M Guehr, X Shen, R Li, T Vecchione, R Coffee, J Corbett, A Fry, N Hartmann, C Hast, K Hegazy, K Jobe, I Makasyuk, J S. Robinson, M Robinson, S Vetter, S Weathersby, C Yoneda, X Wang, and M Centurion. Diffractive imaging of coherent nuclear motion in isolated molecules. Phys. Rev. Lett., 117(15):153002, 2016.

[149] J Yang, X Zhu, T J A Wolf, Z Li, J P F Nunes, R Coffee, J P Cryan, M Gühr, K Hegazy, T F Heinz, K Jobe, R Li, X Shen, T Veccione, S Weathersby, K J Wilkin, C Yoneda, Q Zheng, T. J. Martinez, M Centurion, and X Wang. Imaging cf3i conical intersection

and photodissociation dynamics with ultrafast electron diffraction. Science, 361(6397): 64–67, 2018.

[150] TJA Wolf, DM Sanchez, J Yang, RM Parrish, JPF Nunes, M Centurion, R Coffee, JP Cryan, M Gühr, K Hegazy, et al. Imaging the photochemical ring-opening of 1, 3-cyclohexadiene by ultrafast electron diffraction. arXiv preprint arXiv:1810.02900, 2018.

[151] W H Miller and S J Cotton. Classical molecular dynamics simulation of electronically non-adiabatic processes. Faraday Discuss., 195:9–30, 2016.

[152] H-D Meyer and W H Miller. A classical analog for electronic degrees of freedom in nonadiabatic collision processes. J. Chem. Phys., 70(7):3214–3223, 1979.

[153] S J Cotton and W H Miller. Symmetrical windowing for quantum states in quasi-classical trajectory simulations. J. Phys. Chem. A, 117(32):7190–7194, 2013.

[154] S J Cotton and W H Miller. Symmetrical windowing for quantum states in quasi-classical trajectory simulations: Application to electronically non-adiabatic processes. J. Chem. Phys., 139(23):234112, 2013.

[155] A J Jenkins, K E Spinlove, M Vacher, G A Worth, and M A Robb. The ehrenfest method with fully quantum nuclear motion (qu-eh): Application to charge migration in radical cations. J. Chem. Phys., 149(9):094108, 2018.

[156] D V Makhov, W J Glover, R J Martinez, and D V Shalashilin. Ab initio multiple cloning algorithm for quantum nonadiabatic molecular dynamics. J. Chem. Phys., 141 (5):054110, 2014.

[157] G A Meek and B G Levine. The best of both reps—diabatized gaussians on adiabatic surfaces. J. Chem. Phys., 145(18):184103, 2016.

[158] L Joubert-Doriol, J Sivasubramanium, I G Ryabinkin, and A F Izmaylov. Topologically correct quantum nonadiabatic formalism for on-the-fly dynamics. J. Phys. Chem. Lett., 8(2):452–456, 2017.

[159] L Joubert-Doriol and A F Izmaylov. Variational nonadiabatic dynamics in the moving crude adiabatic representation: Further merging of nuclear dynamics and electronic structure. J. Chem. Phys., 148(11):114102, 2018.

[160] G W Richings and S Habershon. MCTDH on-the-fly: Efficient grid-based quantum dynamics without pre-computed potential energy surfaces. J. Chem. Phys., 148(13): 134116, 2018.

[161] P O Dral, M Barbatti, and W Thiel. Nonadiabatic excited-state dynamics with machine learning. J. Phys. Chem. Lett., 9:5660–5663, 2018.

[162] W-K Chen, X-Y Liu, W Fang, P O Dral, and G Cui. Deep learning for nonadiabatic excited-state dynamics. J. Phys. Chem. Lett., 9:6702, 2018.

[163] I Polyak, G W Richings, S Habershon, and P J Knowles. Direct quantum dynamics using variational gaussian wavepackets and gaussian process regression. J. Chem. Phys., 150(4):041101, 2019.

[164] M Kowalewski, K Bennett, and S Mukamel. Cavity femtochemistry: Manipulating nonadiabatic dynamics at avoided crossings. J. Phys. Chem. Lett., 7(11):2050–2054, 2016.

[165] H L Luk, J Feist, J J Toppari, and G Groenhof. Multiscale molecular dynamics simulations of polaritonic chemistry. J. Chem. Theory Comput., 13(9):4324–4335, 2017.

[166] T E Li, A Nitzan, M Sukharev, T Martinez, H-T Chen, and J E Subotnik. Mixed quantum-classical electrodynamics: Understanding spontaneous decay and zero-point energy. Phys. Rev. A, 97(3):032105, 2018.